Russian Chemical Reviews **81** (1) 1 – 20 (2012) © 2012 Russian Academy of Sciences and Turpion Ltd

DOI 10.1070/RC2012v081n01ABEH004207

Spatial inhomogeneity in crystalline materials and saddle-type congruent melting points in ternary systems

P P Fedorov, I I Buchinskaya

Contents

I.	Introduction	1
II.	Congruent melting points	2
III.	Thermodynamic topological analysis of solid solution crystallization	4
IV.	Phase portraits of solidification for continuous solid solutions in ternary systems	5
V.	Prediction of existence of ternary invariant points	8
VI.	Saddle points in ternary systems of alkaline-earth and rare-earth fluorides	10
VII.	Determination of invariant point coordinates	12
VIII.	Single-crystal growth	15
IX.	Processes occurring during cooling	15
X.	Constitutional undercooling stability of the liquid-solid interface in the vicinity of invariant points of ternary solid solutions	15
XI.	Instability of solidification at maximum and saddle points	16
XII.	Physical properties of crystals with compositions corresponding to saddle points	17
XIII.	Prospects for multicomponent systems	17
XIV.	Conclusions	18

Abstract. Solidification of multicomponent melts to solid solutions is considered in terms of thermodynamic topological analysis. The use of phase portraits of systems for finding congruent melting points (invariant points) is discussed. Methods for predicting the existence of invariant points in ternary systems are considered. An example analysis is presented for two series of fluoride systems ($CaF_2-SrF_2-RF_3$ and $SrF_2-BaF_2-RF_3$, where R are rare-earth elements). The stability of melt crystallization in the vicinity of congruent melting singular points of solid solutions is discussed. The bibliography includes 104 references.

I. Introduction

It was more than one hundred years ago that Schreinemakers published his articles in Zeitschrift für Physikalische Chemie, and these articles appeared extremely fruitful for promoting progress in diverse fields of chemistry and chemical technology. The consideration of evolution of the chemical composition of a two-phase multicomponent system in thermodynamic terms, where one phase has its composition immediately equalized over the volume of the system and the other is removed from equilibrium, gave rise to researches into simple and fractional distillation, primarily in organic multicomponent systems. The application of mathematical tools, such as qualitative theory of differential equations and topology, to approach these problems resulted in the nascent line of research, namely, thermodynamic topological analysis. We have applied the existing investigative tools to single crystal growth *via* directional crystallization. This allowed us not only to discover new families of highly homogeneous optical materials but also to give a new look on the features of crystallization processes, primarily, from the standpoint of process steadiness, and formulate principles for regulating these processes as oscillating ones.

There are many reviews of methods for manufacturing single crystals, in particular, with high chemical, optical, and phase homogeneity (see, *e.g.*, Refs 1 and 2). However, a systematic consideration of this topic in terms of thermodynamic topological analysis has not been carried out.

In melt growth of solid-solution single crystals, the melt and solid phase, in general, have different equilibrium compositions; that is, solid solutions (except for singular (invariant) points) melt and solidify incongruently. This is responsible for variations in composition (and, accordingly, properties) along the length of a crystal. Further, incongruent solidification frequently gives rise to instability of the liquid – solid interface during normal growth or an instability of a step in facial growth as a result of constitutional undercooling. This instability manifests itself in the appearance of dissipative (in particular, cellular and den-

P P Fedorov A M Prokhorov General Physics Institute, Russian Academy of Sciences, ul. Vavilova 38, 119991 Moscow, Russian Federation. Fax (7-499) 135 02 70, tel. (7-499) 503 82 92, e-mail: ppf@lst.gpi.ru
I I Buchinskaya A V Shubnikov Institute of Crystallography, Russian Academy of Sciences, Leninsky prosp. 59, 119333 Moscow, Russian Federation. Fax (7-499) 135 10 11, e-mail: buchinskaya@ifti.ru

Received 14 January 2011
Uspekhi Khimii **81** (1) 1 – 20 (2012); translated by G A Kirakosyan

dritic) structures, which correspond to the spatial chemical inhomogeneity of the as-grown crystal. For eliminating cellular substructure and getting a homogeneous crystal, crystallization rates should be reduced, frequently, to unrealistic values. Getting a solid-solution crystal with a constant concentration along its length requires employing special techniques, such as melt feeding with one component or providing diffusional mass transport of the melt to the liquid–solid interface [Stepanov's technique[3] and its modifications,[4] axial heat-flux-close-to-the-phase-interface growth (AHP methods)[5] and some others]. These techniques are capable of equalizing concentrations along the crystal length, but the stability of the liquid–solid interface remains a problem.

Finding the congruently melting compositions of solid solutions (or compositions nearby) provides a great increase in crystallization rates with retention of quality of crystals and, as a rule, means the creation of a new material (see, *e.g.*, Ref. 6).

For binary solid solutions, the vicinities of points with congruently melting compositions (minima and maxima) are especially advantageous over lightly doped crystals in the context of preparing homogeneous single crystals, for the reason that minor deviations from congruent compositions do not bring about the loss of stability of the liquid–solid interface.[7]

In multicomponent systems, the value of congruent melting points is even greater. According to Bagdasarov's empirical rule,[8] the melt crystallization rates necessary for growing high-quality single crystals decrease on the average by one order of magnitude when the number of components of the system (n) increases by unity. Therefore, invariant points and their vicinities, which do not obey this rule and allow crystallization to be carried out at high rates, are especially attractive.

However, because of the exhausted opportunities of unary and (in part) binary systems as sources of new materials, materials science necessitates going to multicomponent systems.[9] For example, the optimization of praseodymium ion lasing parameters in fluorite solid solution for laser converters in fiber-optic communication systems required growing high-quality single crystals in the $BaF_2-GdF_3-YbF_3-PrF_3$ four-component system.[10] However, as the number of components increases, the total number of systems increases strongly, too. If we take 28 practically valuable inorganic fluorides as components (fluorides of trivalent La, lanthanides, Y, Sc, In, and Bi; divalent Mg, Ca, Sr, Ba, Cd, and Pb; monovalent Li, Na, and K; and tetravalent Zr and Hf), we will obtain 378 binary systems, 3276 ternary systems, and 20475 quaternary systems.[11] In view of the great complexity of studies, it is quite clear that any more or less complete study is impracticable for ternary systems, and all the more so for multicomponent systems. Evidently, there is need for developing and employing methods for predicting and rapidly investigating phase equilibria in ternary and multicomponent systems.

This work is an example application of the thermodynamic topological approach to analysis of solid solutions in ternary fluoride systems with the goal of proving its efficiency in searching for liquidus-surface invariant points. These points are sources of new crystalline materials.

The invariant point problem in ternary and multicomponent systems has been studied in a comprehensive way for liquid–vapour equilibrium[12–17] in the context of optimizing simple and fractional distillation processes. The results can be straightforwardly transferred to crystal–melt equilibrium[18–22] due to the use of the common thermodynamic topological approach.

II. Congruent melting points

Let us consider the formation of congruently melting compositions in multicomponent systems in terms of the phase rule. In the context, congruence is understood as the equality of the compositions of coexisting phases (as is made, *e.g.*, by Storonkin[23]). For three-component and more complex systems, this interpretation of the term differs from the one used by Palatnik and Landau,[24] who understand congruence as the equality of the concentrations of only one component in coexisting phases. Another meaning of congruence is used by Zlomanov.[25]

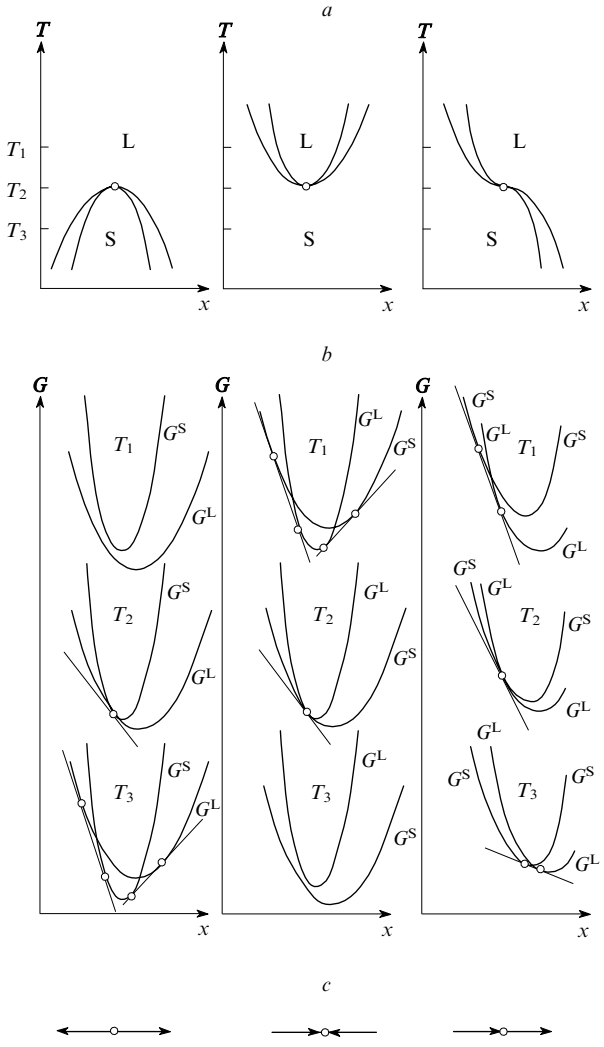


Figure 1. Segments of liquidus and solidus curves (*a*), relationship between the isobaric-isothermal potential curves of a solid phase and a liquid phase at three temperatures (*b*) and phase portraits (*c*) for the formation of maxima, minima and shunts on the melting curves of phases of variable composition in binary systems.

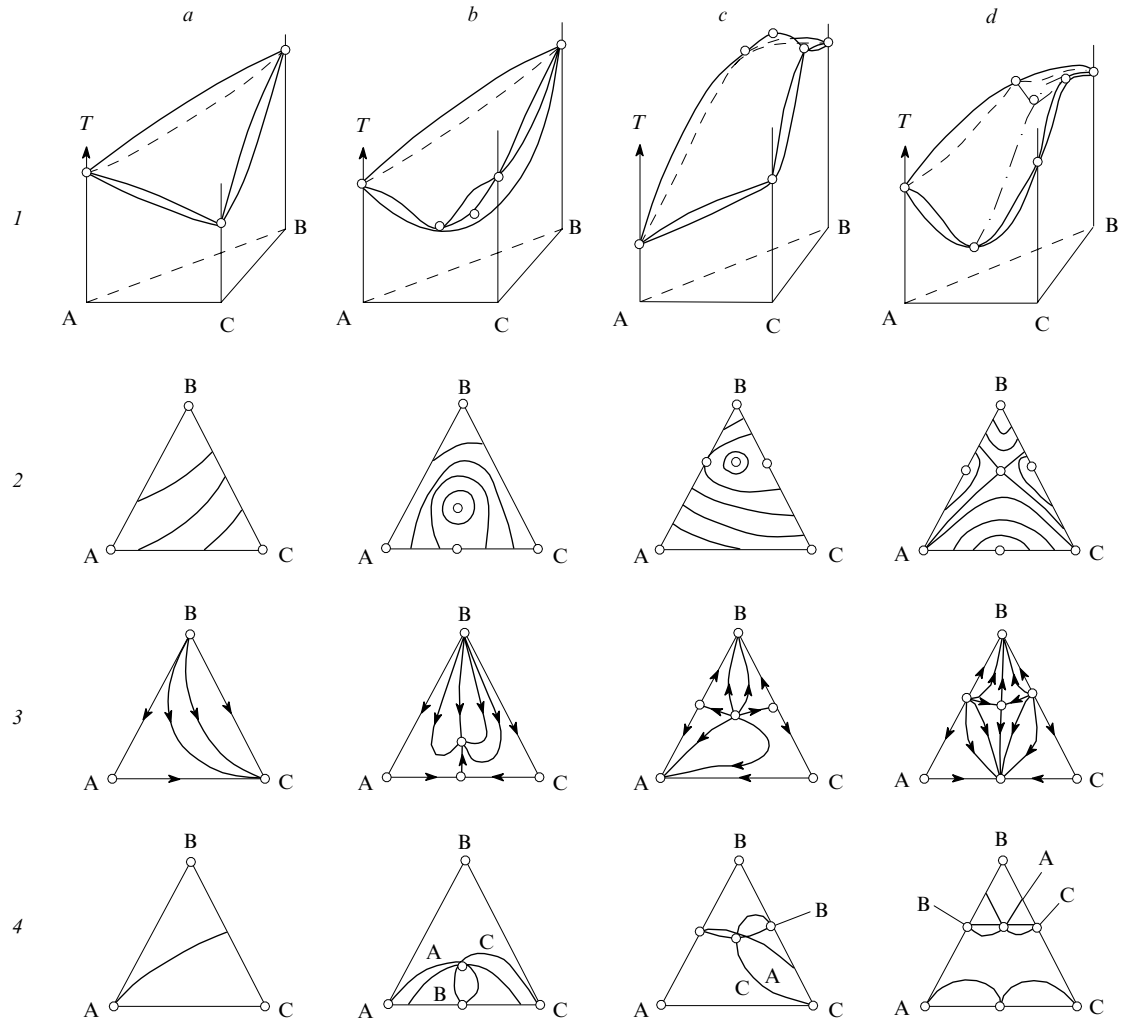


Figure 2. Some suggested types of liquid–solid phase diagrams for ternary systems with continuous solid and liquid solutions in the absence (*a*) and in the presence (*b*–*d*) of congruent melting points on melting surfaces: (*1*) the general view of $T-x$-diagrams, (*2*) liquidus surface projections (lines denote isotherms), (*3*) phase portraits, (*4*) distribution coefficient single-value lines (Serafimov's unit k-lines).[19]

For an n-component system, Kosyakov† proposes the concept of the first, second, etc. order congruence depending on the number of components that have equal concentrations in coexisting phases. The n and $(n-1)$ oder congruence corresponds to complete congruence. Here, we will always mean complete congruence.

The thermodynamic phase rule in the general case reads as

$$f = n + p - \varphi - a,$$

where f is number of degrees of freedom, n is number of components, φ is number of phases in equilibrium, p is number of variable parameters of the state of the system, and a is number of additional constraints imposed on the system (or number of coupling equations existing in the system).[26] Palatnik and Landau [24] have considered this issue using the component concentration matrix concept.

The equality of compositions of coexisting phases in an n-component system gives us $n-1$ coupling equations. Setting $p = 2$ (taking in to account only the temperature and pressure effects), for $\varphi = 2$ we obtain $f = 1$. If pressure is fixed, then $f = 0$. Thus, at a fixed pressure, such a system is characterized by zero degrees of freedom, *i.e.*, is an invariant system: any change in parameters of equilibrium forces the system out of this state. From this, it follows that congruently melting compositions are discrete points in the concentration space, because there is no possibility for concentrations to change provided that the equality of compositions of coexisting phases is held.

In Anosov's fundamental manual,[27] we see a typical error in the description of phase equilibria in ternary systems with minima/maxima in the liquidus surface; this error consists in the statement that there exists a line along which components have equal concentrations in coexisting phases.

In binary systems, three types of congruently melting compositions can exist with the corresponding points on melting curves of solid solutions (Fig. 1) (hereafter, S stands for a solid phase and L for liquid). Minima and maxima on melting curves are well known. Apart from these types of points (which are stable against small changes in parameters

† Unpublished data.

of the state of the system (*i.e.*, are topologically rough [28] or structurally stable points), there can exist non-rough points which are generated by merging minima and maxima and can exist only under a certain fixed pressure.[29] Hereafter, extreme points on melting curves will be referred to as binary extreme points.

From the van der Waals thermodynamic equation [30] for coexisting phases in a binary system under a fixed pressure,

$$\left[\Delta S - \Delta x\left(\frac{\partial S}{\partial x}\right)_{P,T}\right]\mathrm{d}T + \Delta x\left(\frac{\partial^2 G}{\partial x^2}\right)_{P,T}\mathrm{d}x = 0, \qquad (1)$$

where ΔS and Δx are, respectively, the differences between the entropies and concentrations of a crystal and melt, it follows that liquidus and solidus curves merge at extreme points and have a common horizontal tangent.

Ternary systems with congruently melting solid-solution compositions are distinguished by a greater diversity. Apart from minima and maxima, one more type of rough invariant points may appear on solid-solution liquidus surfaces in these systems, namely, a saddle.

Figure 2 displays some representative ternary systems with continuous solid solutions: without extremes (*a*), with a ternary minimum (*b*), with a ternary maximum (*c*) and with a saddle (*d*). In addition, in Fig. 2 *b* there is a binary minimum on side AC; in Fig. 2 *c* there are two binary maxima on sides AB and BC; and in Fig. 2 *d* there are two binary maxima on sides AB and BC and a binary minimum on side AC.

Saddle points were predicted to exist in ternary systems on the surfaces where phases of variable composition coexist as long ago as by Gibbs.[31] They are well known for liquid – vapour equilibria.[14, 32] For crystal – melt equilibria, our works [33 – 39] have only been preceded by scattered reports. We are aware of data on the $Na_2CO_3 - K_2CO_3 - CaCO_3$ system dated 1919 (Ref. 40) and apparently an unrecognized saddle point in the Bi_2Se_3, $Sb_2Te_3//Bi_2Te_3$, Sb_2Se_3 ternary reciprocal system.[41]

Apart from maxima, minima and saddles, the melting surfaces of phases of variable composition in ternary systems can theoretically have a specific bifurcation type of non-rough congruent melting point, that is, the one that exists only under a certain strictly definite pressure. Such points are saddle nodes, that is, points that are generated by merging saddles with maxima or minima on melting surfaces (see Fig. 1).[42] The appearance of such points in real phase diagrams is unlikely.

As follows from van der Waals and Storonkin generalized equation,[23] at a congruent melting point that corresponds to two-phase equilibrium in ternary phase diagrams, the liquidus and solidus surfaces of a solid solution merge (have a common horizontal tangent plane), the compositions of the melt and solid solution coincide and the distribution coefficient is unity for all components $k_i = x_i^S/x_i^L$.

III. Thermodynamic topological analysis of solid solution crystallization

For describing the behaviour of solid solutions during crystallization, we consider a conservative system (*i.e.*, a system with negligible weight loss) with a directional movement of the liquid – solid interface (Fig. 3 *a*), where we assume that diffusion in the solid is nonexistent whereas in the melt (except for the near-surface layer whose thickness is small compared to the melt layer) concentrations are equalized instantaneously (complete mixing occurs). These assumptions correspond with the Pfann approximation.[43] Further, let the concentrations of the crystal and melt correspond to the equilibrium phase diagram. This means that the component distribution coefficients upon crystallization are equal to equilibrium bulk coefficients.

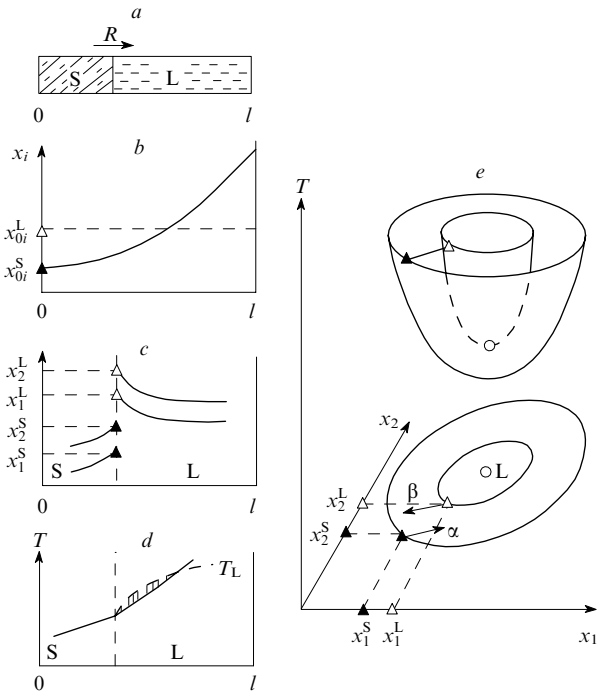


Figure 3. Schematics of directional solidification of a solid solution at rate R (*a*); Pfann's concentration distribution along the crystal length l for component i, $k < 1$ (*b*); component concentrations at the liquid – solid interface (*c*); real solidification temperature and liquidus temperature (T_L) along the ingot length with the hatched constitutional undercooling region (*d*); and liquidus and solidus surfaces of the ternary solid solution in the vicinity of a minimum point with the projection of the section on the concentration plane (*e*);
α is crystallization line and β is diffusion line.[19]

For each component of the system, we may write the mass-balance equation as

$$x_i^S \mathrm{d}g = \mathrm{d}(gx_i^L), \qquad (2)$$

where g is amount of the non-solidified melt, from which it follows that

$$\frac{\mathrm{d}x_i^L}{\mathrm{d}t} = x_i^S - x_i^L = x_i^L(k_i - 1), \qquad (3)$$

where $t = \ln g$. Variable t, which was introduced by Schreinemakers, is an original analogue of time for quasi-equilibrium processes. Integrating this equation on the assumption of a constant distribution coefficient gives us a well-known Gulliver – Pfann equation (Fig. 3 *b*):[43]

$$x_i^S = x_{i0}^L k_i \left(\frac{g}{g_0}\right)^{k_i - 1}. \qquad (4)$$

Here, the subscript zero refers to the initial conditions.

This equation holds both for binary systems and for each component of a ternary or more complex system. Inasmuch as component concentrations (expressed in mole fractions) are related through $\Sigma x_i = 1$, for a ternary system we have set (3) of two differential equations. In the vector representation, this result is written as

$$\frac{d\mathbf{x}^L}{dt} = \Delta\mathbf{x}, \tag{5}$$

where $\Delta\mathbf{x} = \mathbf{x}^S - \mathbf{x}^L$ is composition jump at the crystal–melt interface.

For congruent melting points, $\Delta\mathbf{x} = 0$; that is, phases do not change their compositions upon crystallization. Such points are also referred to as invariant points. (Recall that a straight-line segment connecting the points that represent compositions of phases in equilibrium in the triangular diagram is referred to as a tie-line.) For invariant points, tie-lines transform to points.

Excluding parameter t, we obtain

$$\frac{dx_1^L}{dx_2^L} = \frac{x_1^S - x_1^L}{x_2^S - x_2^L} = \frac{x_1^L(k_1 - 1)}{x_2^L(k_2 - 1)}. \tag{6}$$

This equation was first derived by Schreinemakers.[12] A generalized equation is found in the publications.[23 44]

Differential equation (6) is individual for each particular physicochemical system. This is a nonlinear equation since the difference between the compositions of a solid phase and a liquid phase is a complex function of concentration. The curves characterizing how the melt composition changes during solidification are analogues of distillation lines that describe liquid–vapour equilibrium.[12–14]

Proceeding from Eqs (5) and (6), we can deduce the following properties of melt-composition curves:

— everywhere, except for invariant points, one line passes through one point of the plane (quasi-equilibrium crystallization is a one-way process);

— crystal–melt (solid–liquid) tie-lines are tangents to melt-composition curves.

From the practical point, it is far more convenient to operate with composition variations in a crystal than in melt. Eqn (5) may be rewritten as

$$\frac{d(x_i^S/k_i)}{dt} = \Delta\mathbf{x}_i, \tag{7}$$

to give us crystal-composition lines which we referred to as crystallization lines.[19] The pathways of crystallization lines are close to the pathways of melt-composition lines (in particular, their orientations coincide: melt and crystal compositions change in one direction), although crystallization lines have not solid–liquid tie-lines as tangents.

IV. Phase portraits of solidification for continuous solid solutions in ternary systems

The set of crystallization lines in a triangular diagram provides (in terms of theory of differential equations)[45–47] a phase portrait of the system. In this case, the 'phase'

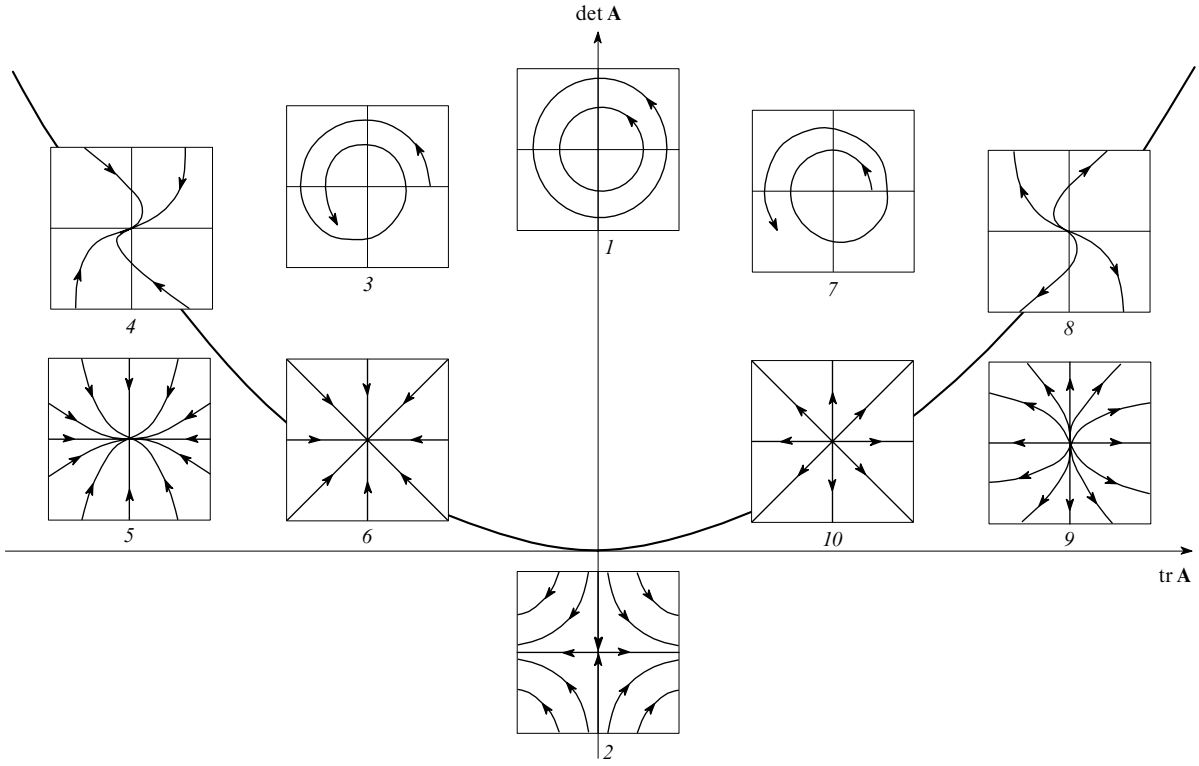


Figure 4. Types of singular points of a set of differential equations in the determinant–trace space ($\det\mathbf{A} = a_{11}a_{22} - a_{12}a_{21}$, $\mathrm{tr}\,\mathbf{A} = a_{11} + a_{22}$).[46]
(*1*) centre; (*2*) saddle; (*3*) stable focus; (*5*) stabe node; (*7*) unstable focus; (*9*) unstable node; (*4*, *6*, *8*, *10*) transition types of singular points; (*3–6*) attractors; and (*7–10*) repellers.

adjective does not relate to the thermodynamic concept of a phase. Some example phase portraits are presented in Fig. 2 (row *3*). We should stress that the phase portraits of a system as set by melt-composition and crystallization lines are topologically equivalent and have invariant points at the same concentrations.

Noteworthy, if we confine ourselves to rough cases, the phase portraits of ternary systems feature only three types of singular points: (1) stable nodes, at which crystallization lines converge; (2) unstable nodes, from which crystallization lines originate; and (3) saddles, in the vicinity of which crystallization lines behave hyperbolically (except for two lines, namely, separatrices which pass through the saddle point). In terms of the number of components, these singular points may be ternary points (a stable ternary node, which is a melting-point minimum, or an unstable ternary point, which is a melting-point maximum; see Figs 2*b*,*c,* respectively), binary points (an example of a binary node is given in Fig. 2*d*, side AC; an example of a binary saddle is in Figs 2*b*,*c*) or unary points (corners of concentration triangles). A unary point is a stable node if addition of both components increases the melting point (Fig. 2*c*; corners A, B) or an unstable node if addition of both components decreases the melting point (Fig. 2*b*, corner B). In case the components added have opposite effects on the melting point, such a corner is a saddle (Fig. 2*a*, corner A; Fig. 2*b*, corners A, C; Fig. 2*c*, corner C).

From theory of differential equations,[45–47] we know that the total number of mathematically allowed types of invariant points is very great. Even for a set of two linear differential equations

$$\begin{aligned} \dot{x}_1 &= a_{11}x_1 + a_{12}x_2\,, \\ \dot{x}_2 &= a_{21}x_1 + a_{22}x_2 \end{aligned} \tag{8a}$$

or (in the matrix form)

$$\dot{x} = \mathbf{A}x, \tag{8b}$$

where **A** is the matrix of coefficients, stable and unstable foci and a centre can exist in addition (Fig. 4). However, the stability conditions for thermodynamic equilibrium exclude the existence of foci and centres for distillation and, accordingly, crystallization lines.[13]

Assuming the possibility of linearizing Eqs (5) and (6) in the vicinity of singular points (which suggests a linear variation in k_i with concentration), we obtain, in this way, nine types of aforementioned singular points. The general ratio between the numbers of these elements in any ternary system is given by Gurikov's equation:[13]

$$2\,C_2 + C_1 + 2 = 2\,N_2 + N_1 + N_0\,, \tag{9}$$

where N is number of nodes, C is number of saddles and subscripts denote the dimension of the element of the concentration triangle in which the relevant point is located.

Gurikov's equation provides the basis for classifying two-phase equilibrium diagrams in ternary systems. Such classifications have been attempted repeatedly since the first decade of the 20th century,[12, 18] but Zharov and Serafimov[14] were the first to report the complete set of variants without gaps (on the assumption that no more than one invariant point exists in each binary or ternary system).

Figure 5 displays 49 kinds of crystallization (distillation) lines and, accordingly, kinds of liquid–vapour and solid–liquid equilibria in ternary systems in the absence of miscibility gaps in all phases and with the existence of a single ternary invariant point ($C_2 + N_2 = 1$) according to Zharov and Serafimov.[14] The basis for classifying the diagrams into groups is the number (M_2) of extremes in partial binaries. Thirty eight types are distinguished as regards the sets of binary and ternary invariant points; some of these types each comprise several kinds (for example, two variants of crystallization line positions correspond to type *21* (one stable binary node and one binary saddle). The diagrams depicted in Figs 2*a*–*d* are equivalent to kinds *1*, *6a*, *10* and *30*, respectively.

Of the melting diagrams of ternary systems with continuous solid solutions studied hitherto, for example, the simplest kind *1* without any extremes is implemented in the diopside $CaMgSi_2O_6$–hedenbergite $CaFe^{II}Si_2O_6$–jadeite $NaAlSi_2O_6$ quasi-ternary system of monoclinic alkali pyroxenes;[48] the CsF–RbF–KF system is of kind *7b* (with one binary minimum), the NaI–KI–RbI system is of kind *36* (three binary minima and one ternary minimum), the Na_2SO_4–K_2SO_4–Rb_2SO_4 system is of kind *37* (three binary minima), the CsBr–RbBr–KBr[49] and SnTe–PbTe–GeTe[50] systems are of kind *21b* (two binary minima), and the Ni–Co–Pd system is likely of kind *20* (with two binary minima and one ternary minimum).[51]

One more basis for classifying two-phase equilibrium diagrams into types is to consider distribution-coefficient lines of equal value on the triangular diagram, in particular, the ones for which $k_i = 1$ (unit k-lines). Zharov and Serafimov's classification[14] has this basis; some examples are given in Fig. 2 (row *4*). The basic properties of these lines are as follows:[14]

— three $k_i = 1$ lines meet at a ternary invariant point, two $k_i = 1$ lines originate from a binary extreme point inward of the triangle, and a single k-line originates from a triangle corner given that this corner is a saddle;

— $k_i = 1$ lines end either at invariant points that involve component i or on the triangle side that corresponds to the zero content of component i.

To some kinds of phase equilibria depicted in Fig. 5, there correspond several variants of unit k-diagrams.

Since Eqs (5) and (6) are actually nonlinear, complex invariant points can exist on the melting surfaces of ternary solid solutions in addition to simple invariant points.

Cases where two invariant points (*e.g.*, a binary point and a unary point or a ternary point and a binary point) coincide, analyzed in detail for liquid–gas equilibria,[14] have been referred to as tangential azeotropes. For solid–liquid equilibria, the relevant term is 'tangential extremes'.[7] Tangential phenomena are invariant; that is, they take place at strictly definite values of an equilibrium parameter, *e.g.*, pressure. In mathematical terms, they correspond to non-rough systems and disappear given that the equilibrium parameter experiences a small change (when the system 'moves').

Zharov and Serafimov[14] suggested that the classification shown in Fig. 5 refers to rough systems. However, the classification comprises non-rough cases. In rough systems, there cannot be separatrices going from a saddle to a saddle.[45] Accordingly, phase portraits *25a* and *38a* shown

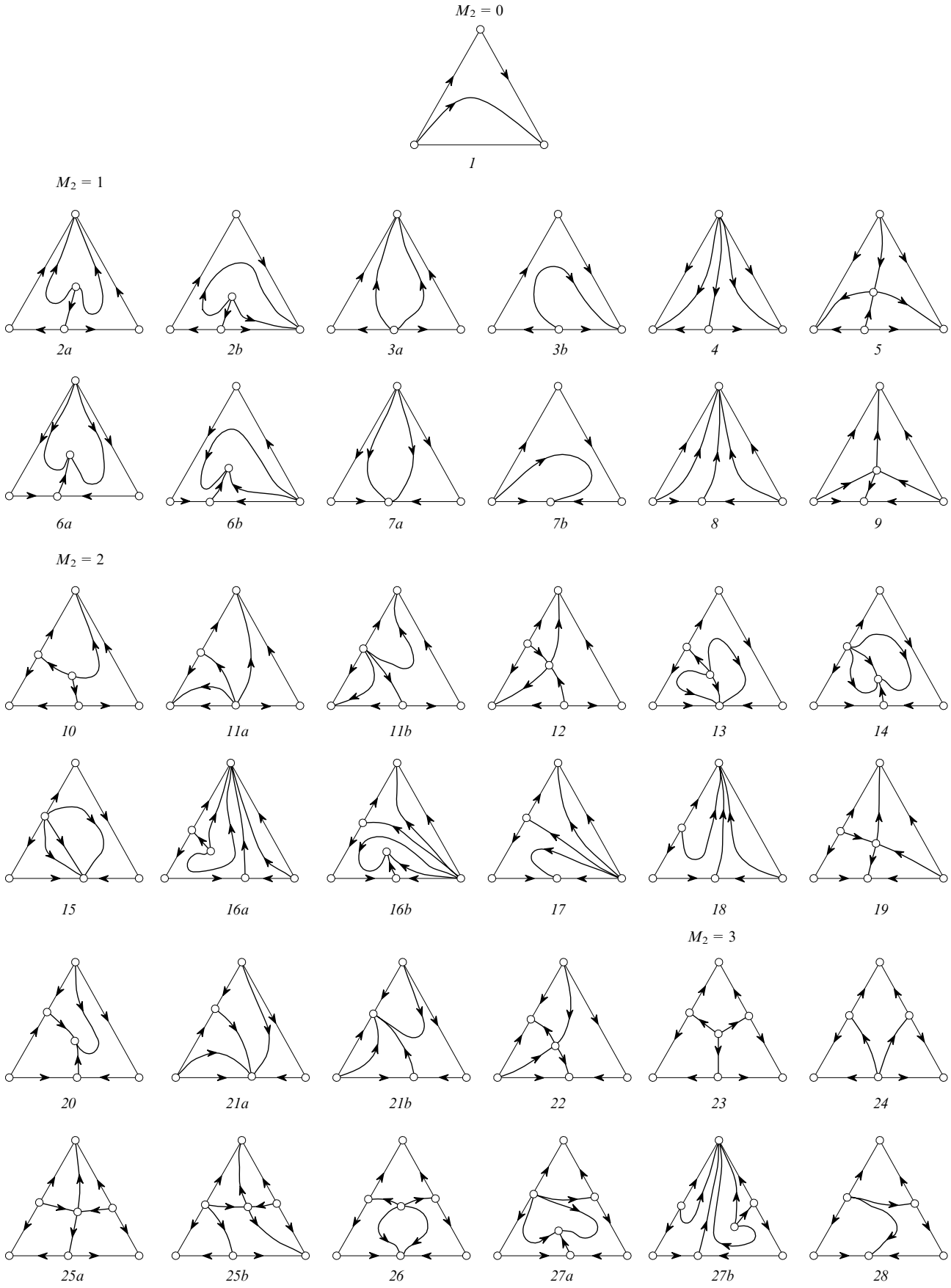


Figure 5. Kinds of crystallization (distillation) diagrams in ternary systems without immiscibility in solid or liquid solutions.[14]

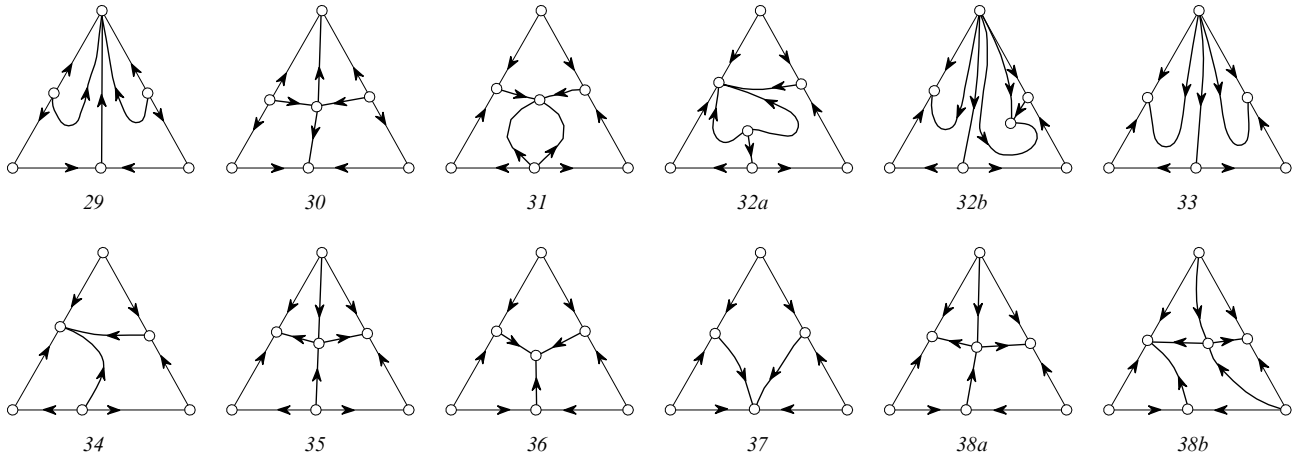


Figure 5 (continued).

in Fig. 5 are unstable, and given small changes in initial conditions, they should transform to the right-hand or left-hand variants of kinds *25b* and *38b*, respectively.

The applicability of the above-described classification to ternary systems is limited by the fact that, in most cases, solid solutions are not continuous and occupy only some portion of the triangular diagram. Only part of one of the phase portraits presented in Fig. 5 is implemented on this concentration field. In particular, for a lithium niobate phase of variable composition in the $Li_2O-MgO-Nb_2O_5$ ternary system (this system is characterized by both a ternary liquidus-surface maximum and a melting-curve maximum in $Li_2O-Nb_2O_5$ binary system[52,53]), the phase portrait corresponds to a fragment of kind *10* (Fig. 6 *a*). The phase portrait for the Tl_2Se-based solid solution in the Tl–Sb–Se system is likely to be of the same kind.[54] The primary crystallization fields of fluorite solid solutions in the $CaF_2-SrF_2-MnF_2$,[55] $NaF-CaF_2-YbF_3$ (Fig. 6 *b*)[56] and $NaF-PbF_2-YbF_3$ (Fig. 6,*c*) systems correspond to fragments of phase portraits of kind *8*, *4* and *11a*,*b*, respectively.

The classification of phase portraits for ternary reciprocal systems, where the concentration space represents a square, has been reported.[57]

V. Prediction of existence of ternary invariant points

In a general case, when one knows the behaviour of binary subsystems, it is difficult to predict the type of a ternary system being based on topological analysis data solely without thermodynamic and/or physicochemical data; the number of possible variants is sufficiently great. However, the following basic inference is possible: given there exists a binary extreme (minimum or maximum), in a general case (except for rare near-tangential extremes), this extreme is not displaced, in either temperature or composition, in response to an attempt to modify it by addition of a third component that dissolves in the initial solid solution; rather, it disappears. In other words, a ternary composition becomes a incongruently melting composition. This is a complete analogy to what occurs when a second isomorphous component is added to an individual substance: the resulting binary alloy, in the general case, melts incongruently, because the melting point transforms into a melting range. In the same way, when having two systems with extremes on the melting curves of binary solid solutions that crystallize in one structural type and are similar in their physicochemical nature (with close values of ionic radii and bond ionicities), we go to a ternary solid solution, extremes will disappear and melting will occur within a temperature range. This case can correspond to kinds *11a*,*b* and *21a*,*b*

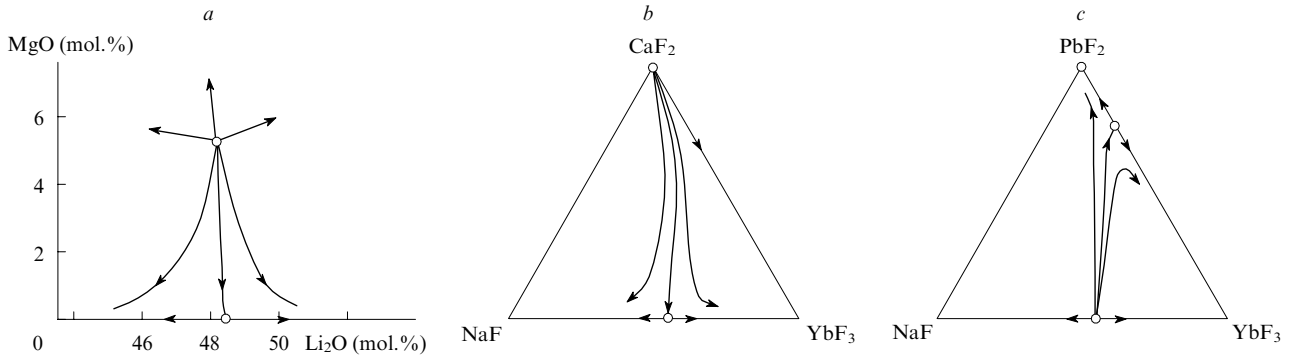


Figure 6. Schematic phase portraits of solid-solution regions in the $Li_2O-MgO-Nb_2O_5$ (*a*), $NaF-CaF_2-YbF_3$ (*b*) and $NaF-PbF_2-YbF_3$ (*c*) systems.

(see Fig. 5). The corresponding polythermal section of the ternary system passing through binary extremes is spindle-shaped.

One such case (with correction for limited solubility) is the $BaF_2-LaF_3-NdF_3$ system (Fig. 7).[58] The $Ba_{1-x}R_xF_{2+x}$ fluorite-type solid solutions that are formed in binary systems have melting maxima at $x = 0.31$ and 0.21 and temperatures of 1484 and 1412 °C for La and Nd, respectively. The triangular diagram displays the primary crystallization fields of fluorite-type solid solutions (F) and tysonite-type solid solutions (T, trigonal crystal system, LaF_3 type). The crystallization temperature range in the ternary fluorite solid solution along the section connecting the binary extremes amounts to 7 °C.

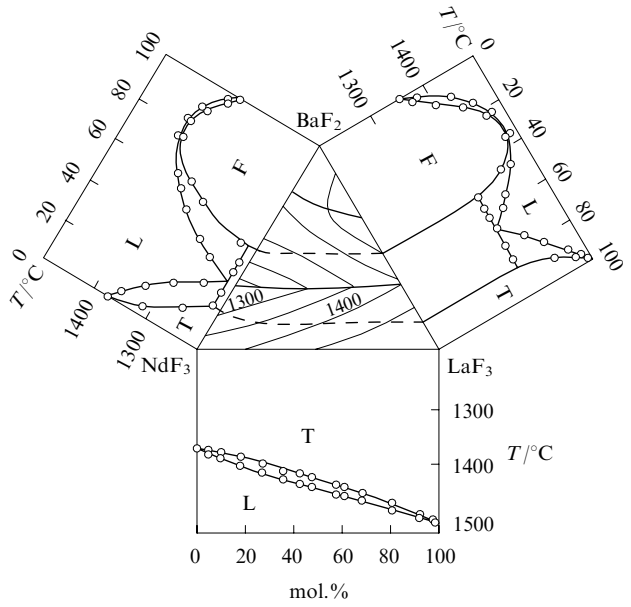


Figure 7. $BaF_2-LaF_3-NdF_3$ phase diagram.[58]
Dashed lines show homogeneity boundaries for phases F and T, and thin lines show isotherms.

As the difference between the melting points of two binary extremes decreases, the liquidus–solidus gap width decreases, the behaviour of the corresponding ternary compositions may insignificantly deviate from the congruent one, and they may be of applied importance. Given that there are two binary extremes on sides A–B and A–C, the appearance of a ternary invariant point is expectable if the properties of components B and C are rather different so that, for example, a binary extreme appears on side B–C between them (kinds *23* and *35* in Fig. 5).

The basic conclusion about a possible appearance of a ternary invariant point on the ternary solid solution surface holds for limited terminal solutions based on component A, including cases where components B and C have different crystal structures.

In the $Al_2O_3-Y_2O_3-Sc_2O_3$ system where a garnet phase has an extensive homogeneity region, for example, a congruent melting point is not formed. When yttrium is replaced by gadolinium (which differs more greatly from scandium in its properties), a maximum was found on melting curves for the garnet phase.[59–61]

There is a rapid method, an analogue of the one described by Zharov and Serafimov,[14] which is very convenient for recognizing the existence of a ternary invariant point. This method is based on Gurikov's equation and consists in the determination of the sign of temperature depression induced by addition of a third component to binary compositions that correspond to extremes. For example, let we have a ternary system with minima P and Q on the melting curves of solid solutions in two binary systems, and let data on the melting character of ternary solid solutions be lacking (Fig. 8 *a*). Corners B and A are unstable nodes, and corner C is a saddle. If, for example, temperature decreases when component C is added to composition P but increases when component A is added to composition Q, then point P is a binary saddle and point Q is a binary node. Thus, we have $N_0 = 2$, $N_1 = 1$ and $C_1 = 1$, and Gurikov's equation (9) takes the form

$$2C_2 + 3 = 2N_2 + 3.$$

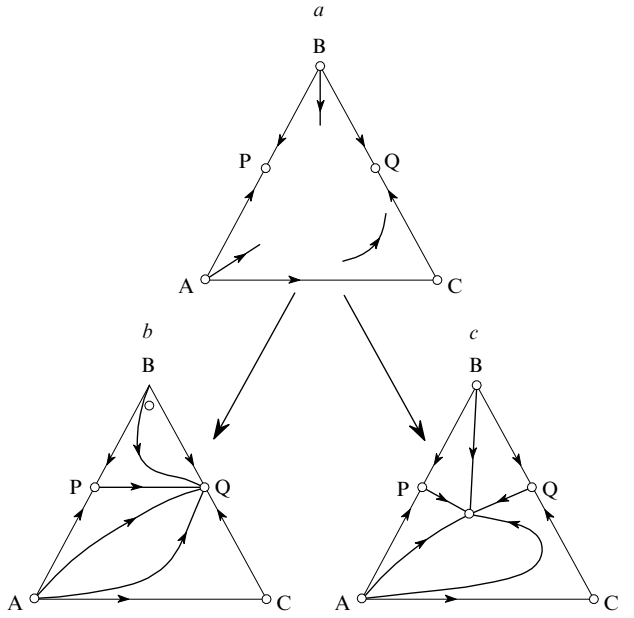


Figure 8. Initial data on binary systems (*a*) and ternary phase portait variants (*b*, *c*).[19]

Since the existence of two ternary invariant points simultaneously is unlikely, we may take that the system under consideration lacks them. The resulting phase portrait of the system in this case is as depicted in Fig. 8 *b*; it corresponds to kind *21b* (see Fig. 5). If the melting point decreases regardless of whether component C is added to composition P or component A is added to composition Q, then both points (P and Q) are binary saddles. If so, $N_0 = 2$, $N_1 = 0$ and $C_1 = 2$, and Eqn (9) becomes

$$2C_2 + 4 = 2N_2 + 2.$$

The only possibility for this equality to be satisfied exists when $C_2 = 0$ and $N_2 = 1$. Thus, there is a ternary extreme (minimum) in the system; the phase portrait is shown in Fig. 6 *c* and corresponds to kind *20* (see Fig. 5).

VI. Saddle points in ternary systems of alkaline-earth and rare-earth fluorides

The probability of a ternary invariant point (namely, a saddle) to appear is especially high in ternary systems where there are two binary minima and one maximum or *vice versa*. The $MF_2-M'F_2-RF_3$ systems of fluorides of divalent elements (M, M′) and rare-earth elements (R) are just such the promising cases. The $M_{1-x}R_xF_{2+x}$ fluorite solid solutions are characterized by melting-curve maxima for many rare-earth elements.[9, 62, 63] Meanwhile $MF_2-M'F_2$ systems in some cases, namely, in the CaF_2-SrF_2,[64, 65] SrF_2-BaF_2,[66] SrF_2-CdF_2 (Refs 6, 67) and CdF_2-PbF_2 systems[67, 68] feature continuous fluorite-type solid solutions with minima on the liquidus curves. In the CaF_2-BaF_2 system,[69] extensive component-based solid solutions have a miscibility gap; the melting curves of the BaF_2-based solid solution, however, have a minimum point.

The prediction[19] of the existence of saddle invariant points in such the systems has been embodied:[33–38] several tens of saddle points exist in the $CaF_2-SrF_2-RF_3$, $BaF_2-SrF_2-RF_3$ and $PbF_2-CdF_2-RF_3$ systems.

The experimental results obtained in studying some phase diagrams with ternary saddles are displayed in Figs 9–12 (see also Figs 1 and 2 in the electronic appendix). The investigative tools were differential thermal analysis (DTA) with a special feeder design that provided a manifold enhancement in the precision of the experiment and X-ray powder diffraction of annealed and quenched samples.

In the CaF_2-SrF_2 system, there is continuous solid solution $Ca_{1-y}Sr_yF_2$ with a minimum at 40 mol.% SrF_2 ($y = 0.40$) and 1362 °C. The SrF_2-LaF_3 system is a eutectic type (the eutectic coordinates are 70 mol.% LaF_3, 1450 °C) with limited terminal solid solutions. The maximum on the melting curve of the $Sr_{1-x}La_xF_{2+x}$ fluorite solid solution exists at 31 mol.% LaF_3 and 1570 °C. The CaF_2-LaF_3 system is also a eutectic type (the eutectic coordinates are 58 mol.% LaF_3, 1311 °C), and there are no maxima on the melting curves of the solid solution. In the $CaF_2-SrF_2-LaF_3$ ternary system, $(Ca_{1-y}Sr_y)_{1-x}La_xF_{2+x}$ solid solution (phase F in Figs 9–11) is formed due to heterovalent isomorphous substitutions. Sections that pass through the LaF_3 corner demonstrate that liquidus and solidus curves change systematically in response to changing the calcium : strontium ratio from curves with maxima through curves with a trunk (having both maxima and minima) to curves with monotonous temperature variation. The inspection of liquidus-surface isotherms (see Fig. 10*a*) allowed the saddle point to be located at 16 ± 3 mol.% LaF_3, 7 ± 3 mol.% SrF_2, and 1382 ± 5 °C. The smooth

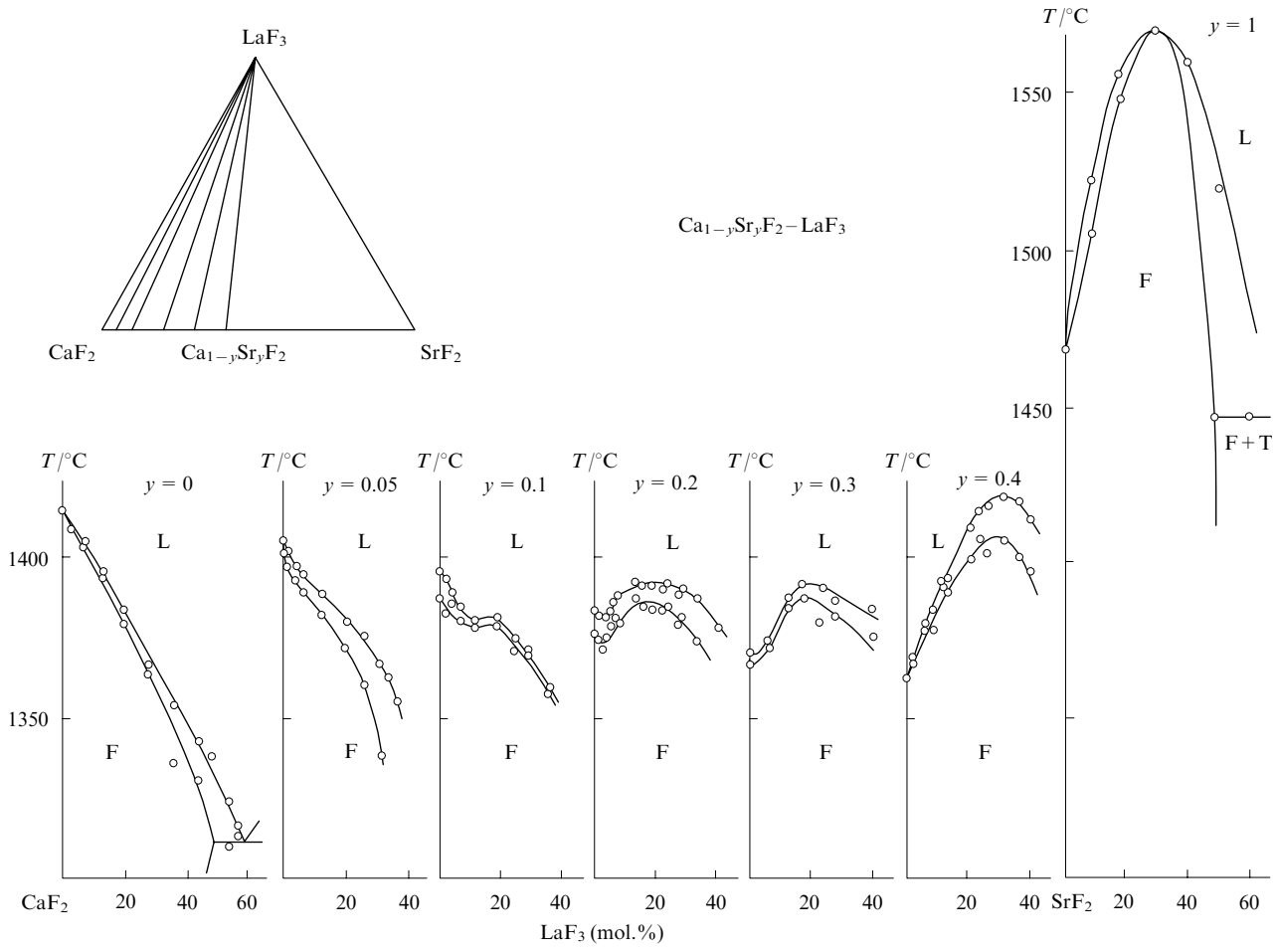


Figure 9. Polythermal sections studied in the $CaF_2-SrF_2-LaF_3$ system.[36, 37]
Circles are DTA data, L is melt and F is $(Ca_{1-y}Sr_y)_{1-x}La_xF_{2+x}$ fluorite-type solid solution.

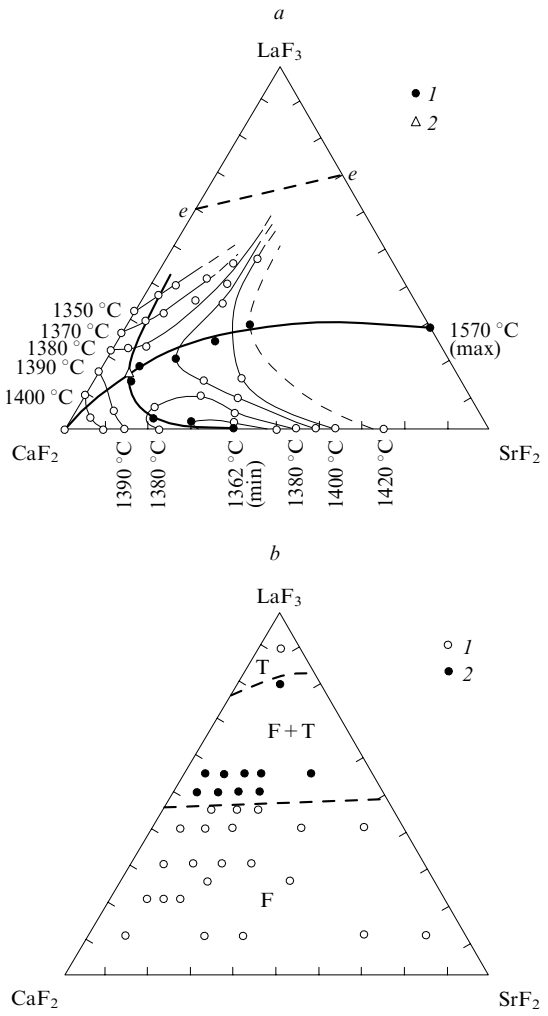


Figure 10. Projection of the primary crystallization surface of $(Ca_{1-y}Sr_y)_{1-x}La_xF_{2+x}$ solid solution (*a*) (thin lines show isotherms/°C; the thin dashed line shows the isotherm for which experimental data are lacking; the thick dashed line is the line of joint crystallization of two solid phases; (*1*) extreme points on the liquidus curves for binary systems and polythermal sections, (*2*) saddle point, and *e* eutectics in binary systems); and the 1100 °C isothermal section in the $CaF_2-SrF_2-LaF_3$ system (*b*) (T is LaF_3-based tysonite solid solution, (*1*) single-phase samples, and (*2*) two-phase samples).

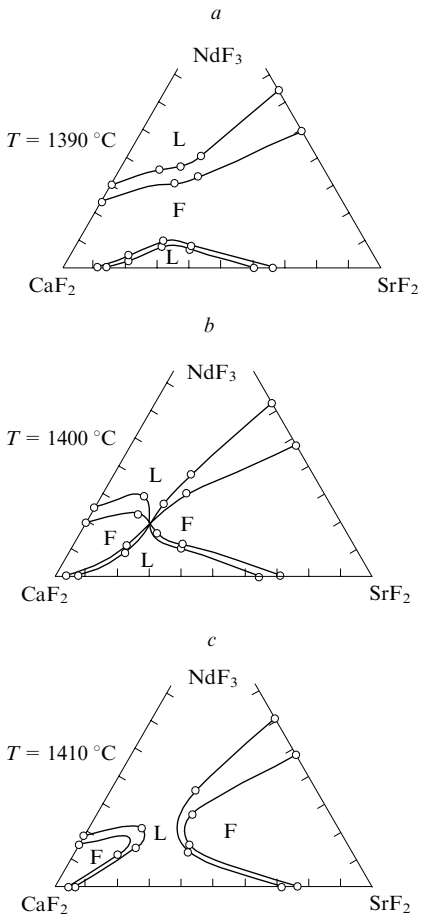


Figure 12. Isothermal sections in the $CaF_2-SrF_2-NdF_3$ system at 1390 °C (*a*), 1400 °C (the saddle-point temperature) (*b*) and 1410 °C (*c*).[35,37] For notations, see Figs 9 and 10.

relief of the liquidus surface in the vicinity of this point makes it difficult to determine its coordinates with high accuracy. On the isothermal section that passes through a saddle point (see Fig. 11 *b*), the solid-solution and melt phase fields merge so that the boundary curves of the single-phase fields meet at this point and have no common tangents. A rise in temperature leads to cutting of the single solid solution field F due to the merge of two melt

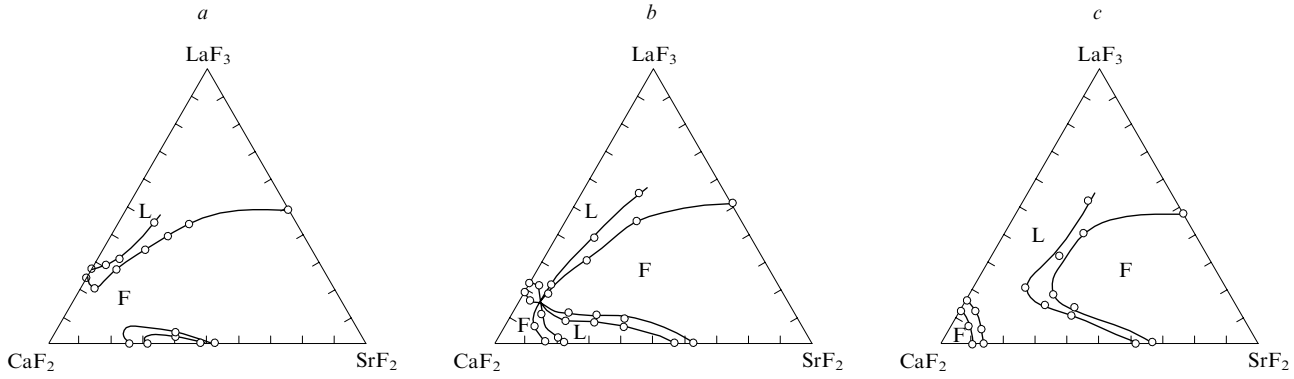


Figure 11. Isothermal sections in the $CaF_2-SrF_2-LaF_3$ system at 1370 °C (*a*), 1382 °C (the saddle-point temperature) (*b*) and 1390 °C (*c*). For notations, see Figs 9 and 10.

fields L.‡ The pathway for crystallization lines for the fluorite solid solution in this system corresponds to a fragment of a kind *19* phase portrait (see Fig. 5).

The $CaF_2-SrF_2-NdF_3$ system (see Fig. 12) is fairly analogous to the lanthanum fluoride-containing system. The $CaF_2-SrF_2-YbF_3$ system has a slightly worse convergence of some of the sections studied,[37] probably because ytterbium partially reduced to the divalent state during the experiment. However, the existence of a saddle point on the solid-solution liquidus surface is undoubtful. The pathway for crystallization lines corresponds to a fragment of a kind *9* phase portrait (see Fig. 5).

The $BaF_2-SrF_2-LaF_3$ system, where there is a saddle point on the crystallization surfaces of fluorite solid solution,[38] corresponds to a fragment of a kind *30* phase portrait (see Fig. 5), because a minimum appears on melting curves in the BaF_2-SrF_2 system and maxima appear in the BaF_2-LaF_3 and SrF_2-LaF_3 systems.

Data on the $PbF_2-CdF_2-RF_3$ system are presented in Figs 1 and 2 of the electronic appendix. Interpolation enables the conclusion that, in this series, saddle points on the melting surfaces exist for R = Tb–Lu or Y.[33, 34]

VII. Determination of invariant point coordinates

Let us dwell on an important applied problem of how to search for compositions of invariant points in ternary systems (and how to find them).

Search methods may be grouped as follows:

(1) studies of phase diagrams;

(2) studies of the crystallization line field;

(3) studies of distribution coefficients as a function of concentration;

(4) studies of crystal perfection (regions where cellular substructure disappears).

In studying melting diagrams, an experiment gives data on the liquidus and solidus temperatures for some number of compositions, as a rule along certain concentration sections (see Fig. 9). Using experimental data, one can fit liquidus and solidus surfaces and, in this way, obtain the coordinates of extremes and saddles. This fitting can be carried out either with the use of thermodynamic models or formally, for example, by polynomials, splines and so on. In the last case, it is pertinent that fitting equations should have common horizontal tangents at invariant points. Example fittings of melting-point surfaces for solid solutions have been carried out for $CaF_2-SrF_2-LaF_3$ system [37] and the $SrF_2-BaF_2-LaF_3$ system.[38]

Difficulties in experimental studies of phase equilibria shoud also be taken into account, in particular, the specifics of interpreting thermoanalytical curves for monovariant phase transformations (*i.e.*, those passing within a temperature range). It is advisable to equate solidus temperatures to the onset temperatures of peaks on heating curves and liquidus temperatures to the onset temperatures of peaks on cooling curves. Two effects should also be kept in mind: on the one hand, possible melt undercooling [70] (fortunately, for fluorite solid solutions, undercooling is ignorable in most cases [34, 37]) and, on the other, underestmation of solidus temperatures because of a concentration inhomogeneity of solid solution samples. Both are systematic effects.

Let us proceed with methods for determining crystallization lines. When directional crystallization fulfills the Pfann assumptions (equilibrium at the solid–liquid interface, full equalization of concentrations over the melt volume and the absence of diffusion in solid), then concentration variation along the crystal length gives a crystallization-line segment. A necessary (but in general insufficient) condition for these assumptions to hold is the fulfillment of the Pfann distribution (4) along the crystal length for all three components. Required determinations are time-consuming, and it is far easier to confine the search stage to determinations of compositions in the initial and end portions of the crystal. Both Czochralski and Bridgman growth techniques can be used.

Frequently, compositions are not derived from chemical analysis; rather, some property is used for which the concentration dependence is known or can be calculated. Of such the properties, we can mention refractive indices, unit cell parameters, and density. Inasmuch as we consider the case of three-component systems, values of at least two properties should be at hand. One property does not determine the composition, and the coincidence of one parameter in the initial and end portions of the crystal is a necessary but insufficient condition of the equality of compositions.

The compositions of the initial and end portions of the crystal give a segment in the concentration triangle, and the less the curvature of the crystallization line, the better the goodness of fit of the crystallization-line segment by this segment. One more segment appears when we consider the compositions of the parent melt and the initial portion of the crystal. If solidification occurred in the quasi-equilibrium mode, this segment is solid–liquid equilibrium tie-line, which is a tangent to the melt-composition line, but not to crystallization lines. Thus, the points corresponding to the compositions of the parent melt and the initial and end portions of the crystal, in general, give two segments (Figs 13 and 14). The combination of these segments gives two topologically equivalent vector fields, and each field can be used in searching for invariant points.

The applicability range of the simplest successive approximation method [71] to the determination of an extreme composition follows from inspection of Fig. 13, as follows: taking some parent melt composition, determine the composition of the first crystal portion; setting that this composition is closer to the extreme, take it as the initial one; and do so on until the compositions of the initial and end crystal portions coincide (to the accuracy of analysis). The successive approximation method is operative only for maxima; for minima, following this way we will go away from the invariant point (in this case, the method is easy to modify); for a saddle, in general, we will pass by. This method well applies to binary systems, because all segments lie on one concentration line, and it is only necessary to catch the inversion of direction. Tanaka *et al.*[72] more accurately determined the maximum point position (YB_{62}) for a congruently melting phase, whose ideal formula is YB_{66}, just in this way.

Concentration series provide a more general method.[60] Even when compositions of the initial and end portions of crystals are only determined, this method gives a general

‡ Figure 11 *b* corresponds to the embodiment of Fig. 7 from Gibbs 'Gleichgewicht der heterogenen Substanzen' (Ref. 31, p. 129), and Figs 11 *a* and 11 *c* correspond to Fig. 7 *a* from the French language translation of this book (Ref. 31, p. 519).

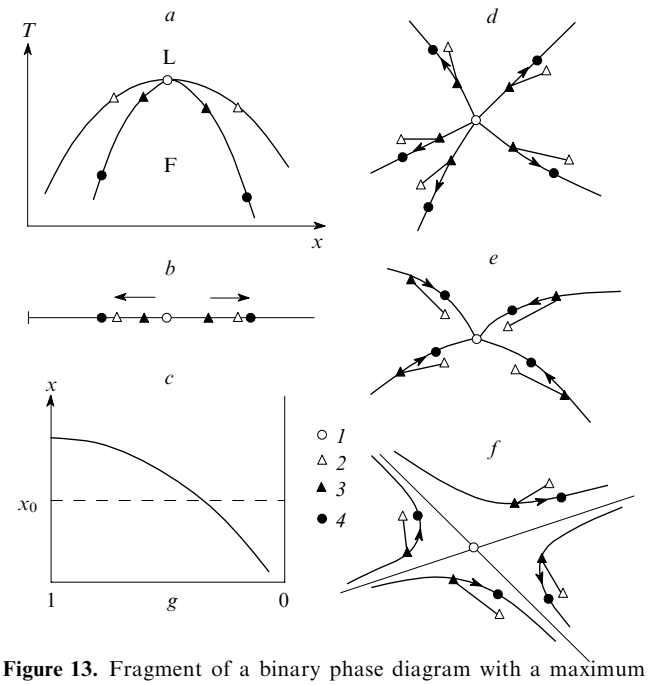


Figure 13. Fragment of a binary phase diagram with a maximum on the melting curve (*a*), phase portrait (*b*) and the composition of a crystal grown under the conditions of the Pfann approximations with $k > 1$ (g is unsolidified melt fraction) (*c*), and the phase portraits of a maximum (unstable node) (*d*), a minimum (stable node) (*e*) and a saddle (*f*) in ternary systems with the compositions indicated for: invariant points (*1*), points corresponding to initial melt compositions (*2*), initial (*3*) and end (*4*) portions of the crystal.[19]

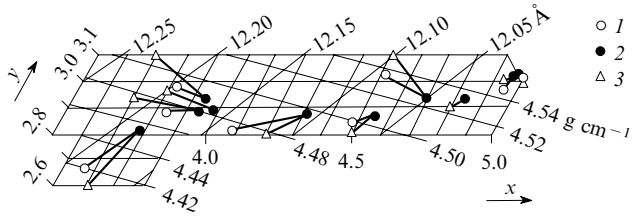


Figure 14. Composition–density (g cm^{-3})–unit cell parameter diagram (Å) for the $Y_2O_3-Al_2O_3-Sc_2O_3$ system with the compositions indicated for Czochralski-grown $Y_yAl_xSc_{8-x-y}O_{12}$ yttrium scandium aluminium garnet crystals.[60]
(*1*) As-batch composition, (*2*) composition of the upper crystal portion and (*3*) composition of the lower crystal portion.

view of the crystallization field. Usually, the concentration series method is combined with the successive approximation method. The composition corresponding to the congruent melting (maximum) point of a phase of variable composition with the nominal composition $La_3Ga_5SiO_{14}$ (langasite) was determined in this way.[73] The resulting fragment of the phase portrait corresponds to Fig. 13 *d*. Provisionally, the maximum point position on the liquidus surface was determined by thermal analysis.[74]

Apart from the heavy curvature of crystallization lines, one more danger of using exclusively initial and end concentrations in crystals consists in a possibility of undercooling and rapid growth of the initial crystal portion with non-equilibrium capture of components. In this context, the Czochralski method is preferred to Bridgman growth. One more problem may be an insufficient accuracy of composition determinations, especially when the crystal is inhomogeneous because of cellular substructure.

An example experimental analysis of the crystallization field is found[61] for the garnet solid solution in the $Y_2O_3-Al_2O_3-Sc_2O_3$ system (see Fig. 14). The Czochralski growth method was used; the composition was derived from densities and unit cell parameters. A maximum exists in the $Y_2O_3-Al_2O_3$ binary system with the composition very close to the $Y_3Al_5O_{12}$ stoichiometry; in the ternary system, there are no invariant points.

Numerous assays of rocks allowed crystallization lines to be sketched in the system of monoclinic alkali pyroxenes.[48]

One more method for the determination of invariant point compositions may be to construct fitting surfaces of distribution coefficient versus concentration dependences $k_i(x_1,x_2)$ and then analyze Serafimov's unit k-lines, finding their meeting points. The initial data set for the calculations may be, for example, the compositions of the parent melt and the initial portion for a series of crystals.

Lastly, once the concentration field of planar growth is identified as a result of growing a series of crystals (for transparent crystals, this can be done optically without carrying out time-consuming determination of compositions), a invariant point may be assumed to lie in the centre of this field. Sorokin *et al.*[75] used just this method to more accurately determine the position of the minimum point on the melting curve for $Cd_{1-x}Pb_xF_2$ solid solution. However, the reliability of the method is not high.

Interpolation was the main method we used for preparing optical single crystals with compositions corresponding to the vicinities of saddle points in the series of

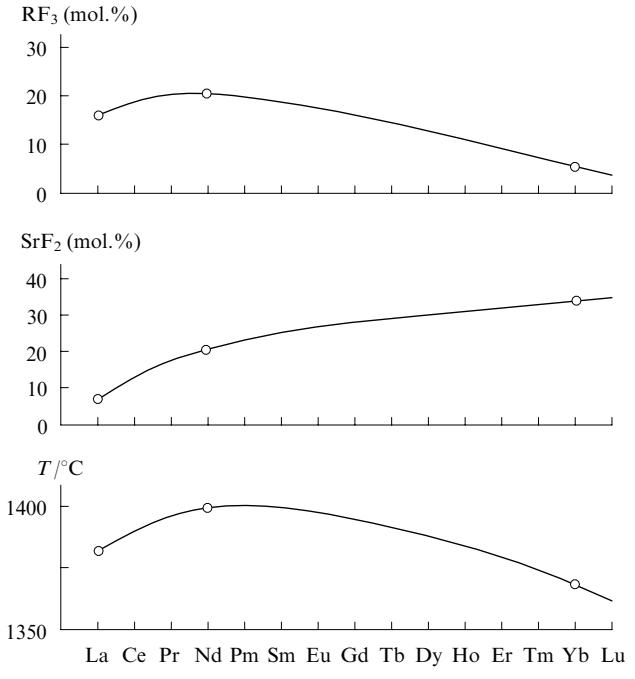


Figure 15. Interpolation plots of saddle point coordinates for $CaF_2-SrF_2-RF_3$ systems.[37]
Symbols denote experimental datapoints.

Table 1. Properties of crystals that correspond to saddle-point compositions on the melting surfaces of ternary solid solutions in $CaF_2-SrF_2-RF_3$ systems.

R	Composition	Molecular weight	Unit cell parameter a/Å	Density /g cm^{-3}		Melting point /°C	Refractive index	Thermal conductivity /W m^{-1} K^{-1}	
				experiment	X-ray			at 50 K	at 300 K
La	$Ca_{0.77}Sr_{0.07}La_{0.16}F_{2.16}$ (see [a])	100.28	5.569	–	3.86	1382 [a]	1.469 [a]	2.03	2.16
Ce	$Ca_{0.70}Sr_{0.11}Ce_{0.19}F_{2.19}$ (see [a])	105.94	5.592	–	4.02	1390 [a]	1.479 [a]	1.87	2.37
Pr	$Ca_{0.65}Sr_{0.15}Pr_{0.20}F_{2.20}$ (see [a])	109.19	5.595	–	4.14	1395 [a]	1.479 [a]	1.31	1.96
Nd	$Ca_{0.58}Sr_{0.21}Nd_{0.21}F_{2.21}$ (see [a])	113.93	5.592	–	4.33	1400 [a]	1.483 [a]	–	–
Sm	$Ca_{0.56}Sr_{0.26}Sm_{0.18}F_{2.18}$	113.72	–	–	–	1402 [b]	–	1.28	1.71
Gd	$Ca_{0.56}Sr_{0.28}Gd_{0.16}F_{2.16}$	113.92	5.597	–	4.29	1399 [b]	–	–	–
Tb	$Ca_{0.56}Sr_{0.295}Tb_{0.145}F_{2.145}$	112.09	5.588	–	4.27	1396 [b]	–	1.07	1.69
Dy	$Ca_{0.555}Sr_{0.305}Dy_{0.14}F_{2.14}$	112.38	–	–	–	1392 [b]	–	(0.88)	(2.04)
Ho	$Ca_{0.56}Sr_{0.32}Ho_{0.12}F_{2.12}$	110.56	5.593	4.21	4.18	1385 [b]	–	1.04	1.75
Er	$Ca_{0.56}Sr_{0.325}Er_{0.115}F_{2.115}$	107.08	5.578	4.18	4.22	1381 [b]	–	1.09	1.74
Tm	$Ca_{0.57}Sr_{0.33}Tm_{0.10}F_{2.10}$	108.56	5.581	4.10	4.15	1376 [b]	–	1.36	1.83
Yb	$Ca_{0.60}Sr_{0.34}Yb_{0.06}F_{2.06}$ (see [a])	103.36	5.571	–	3.96	1370 [a]	1.445	2.35	2.30
Lu	$Ca_{0.61}Sr_{0.35}Lu_{0.04}F_{2.04}$	100.88	–	–	–	1365 [b]	–	–	–
	$Ca_{0.6}Sr_{0.4}F_2$ (see [c, d])	97.10	5.564	–	3.86	1362 [c]	–	–	–
						1373 [d]	–	–	–

[a] Ref. 37; [b] interpolation; [c] Ref. 76; [d] Ref. 65.

$CaF_2-SrF_2-RF_3$ and $BaF_2-SrF_2-RF_3$ systems. Of the first series, phase diagrams were studied for three systems (R = La, Nd, and Yb); in particular, saddle point coordinates were determined (see above). This was sufficient for constructing composition versus R^{3+} ionic radius plots and for predicting saddle point coordinates in the other systems (Fig. 15, Table 1). The experimentally determined melting point of the saddle point in the gadolinium system coincided (±5 °C) with the estimation.

In the $BaF_2-SrF_2-RF_3$ series, a phase diagram has been studied experimentally only for the system with LaF_3. Additional data were gained from the synthesis of a crystalline laser medium in the $BaF_2-SrF_2-YbF_3$ system. When 5 mol.% YbF_3 was added to the composition corresponding to the minimum point in the BaF_2-SrF_2 system, melt-grown crystals had cellular structure (see Fig. 3 in the electronic appendix). When the concentration was decreased to 3 mol.%, laser quality crystals were grown. This information was sufficient for estimating saddle point positions over the entire series of $BaF_2-SrF_2-RF_3$ systems proceeding from the suggested linear dependence of the coordinates on the R^{3+} ionic radius. The results of interpolation are given in Table 2. Single crystal growth data support them.

Figure 16 displays the compositions of saddle points on triangular diagrams for the series of $CaF_2-SrF_2-RF_3$ and $BaF_2-SrF_2-RF_3$ systems. Interestingly, the data for the first series of systems fall on the line that originates from a minimum point in the SrF_2-CaF_2 system and is extrapolated to the CaF_2 corner (*i.e.*, the line connecting a stable node and an unstable node in the phase portraits of ternary systems). For $SrF_2-BaF_2-RF_3$ systems, the curve origi-

Table 2. Properties of crystals that correspond to saddle-point compositions on the melting surfaces of ternary solid solutions in $SrF_2-BaF_2-RF_3$ systems.

R	Composition	Molecular weight	Unit cell parameter a/Å	Density /g cm^{-3}		Melting point /°C	Thermal conductivity /W m^{-1} K^{-1}	
				experiment	X-ray		at 50 K	at 300 K
La	$Sr_{0.16}Ba_{0.54}La_{0.30}F_{2.30}$ (see [a])	173.55	6.037	5.23 ± 0.04	5.24	1455 [a]	0.95	1.31
Ce	$Sr_{0.17}Ba_{0.555}Ce_{0.275}F_{2.275}$	172.87	6.031	5.23 ± 0.03	5.24	–	0.79	1.22
Pr	$Sr_{0.185}Ba_{0.565}Pr_{0.25}F_{2.25}$	171.77	–	5.24 ± 0.03	–	–	0.84	1.32
Nd	$Sr_{0.20}Ba_{0.58}Nd_{0.22}F_{2.22}$	171.08	–	5.26 ± 0.07	–	–	0.88	1.31
Sm	$Sr_{0.22}Ba_{0.60}Sm_{0.18}F_{2.18}$	170.15	–	5.18 ± 0.03	–	–	1.05	1.47
Gd	$Sr_{0.23}Ba_{0.64}Gd_{0.13}F_{2.13}$	168.95	6.037	5.13 ± 0.04	5.10	–	2.02	1.65
Tb	$Sr_{0.26}Ba_{0.65}Tb_{0.09}F_{2.09}$	166.05	6.045	4.97 ± 0.03	4.99	–	2.96	1.88
Dy	$Sr_{0.27}Ba_{0.66}Dy_{0.07}F_{2.07}$	165.00	–	4.96 ± 0.03	–	–	3.47	2.04
Ho	$Sr_{0.28}Ba_{0.66}Ho_{0.06}F_{2.06}$	164.20	6.049	4.84 ± 0.03	4.93	–	4.72	2.16
Er	$Sr_{0.29}Ba_{0.66}Er_{0.05}F_{2.05}$	163.35	6.050	4.85 ± 0.03	4.90	–	5.51	2.23
Tm	$Sr_{0.30}Ba_{0.66}Tm_{0.04}F_{2.04}$	162.44	6.066	4.85 ± 0.03	4.83	–	6.93	2.38
Yb	$Sr_{0.325}Ba_{0.645}Yb_{0.03}F_{2.03}$	160.81	6.0435	4.96 ± 0.09	4.84	–	6.38	2.28
	$Sr_{0.34}Ba_{0.66}F_{2.30}$ (see [b])	158.42	6.064 [c]	–	4.72	1305 [b]	18.4	3.14

[a] Ref. 38; [b] Ref. 66; [c] interpolation.

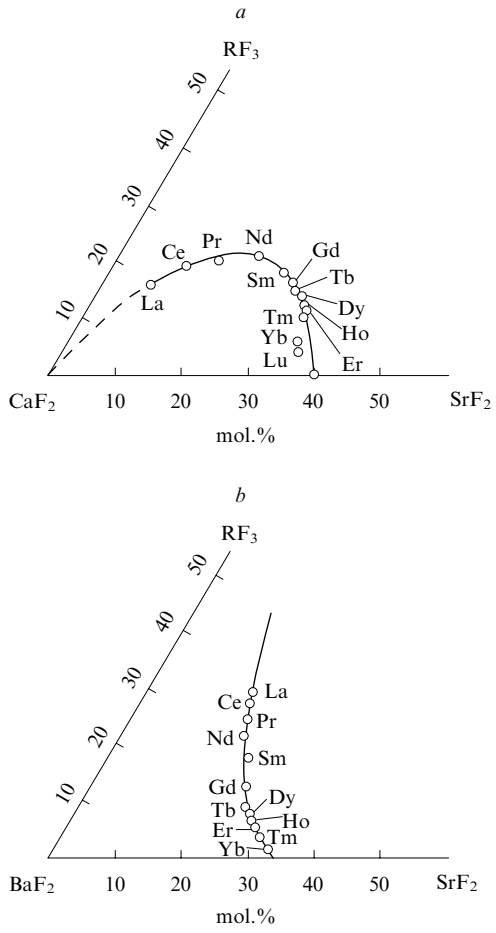


Figure 16. Saddle point compositions on the triangular diagram for $CaF_2-SrF_2-RF_3$ (*a*) and $BaF_2-SrF_2-RF_3$ (*b*) systems.

nates from a minimum point in the $MF_2-M'F_2$ system and is extrapolated to the RF_3 corner (that is, the line connects two stable nodes of the corresponding phase portraits). Apparently, the same situation exists in the series of $PbF_2-CdF_2-RF_3$ systems.

VIII. Single-crystal growth

The prediction served to grow complete series of single crystals with compositions corresponding to the concentration vicinities of saddle points in the rows of $CaF_2-SrF_2-RF_3$ [37, 77–81] and $BaF_2-SrF_2-RF_3$ systems. Single crystals were grown by vertical directional crystallization. An evacuated chamber was used inside which a fluorinating (CF_4) atmosphere was created for suppressing pyrohydrolysis.[78] The initial materials used were chemicals purified by fusion in a fluorinating atmosphere. Graphite resistance heaters and graphite multicellular crucibles were used.

Photographs of some grown crystals are seen in Fig. 4 of the electronic appendix. These crystals are free of cellular structure; some have striations. Figure 17 shows a photograph of a $Ca_{0.60}Sr_{0.34}Yb_{0.06}F_{2.06}$ single crystal, which is an efficient active medium for IR lasers.[77]

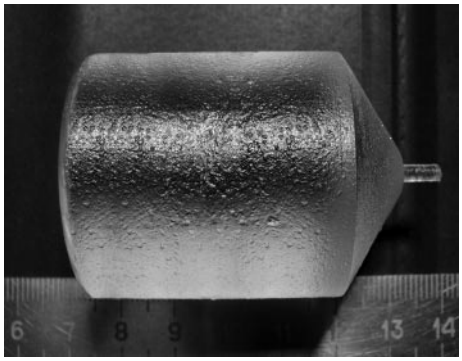


Figure 17. $Ca_{0.60}Sr_{0.34}Yb_{0.06}F_{2.06}$ single crystal is a medium for IR lasers.[77]

IX. Processes occurring during cooling

We should stress that our analysis refers exclusively to searching for optimal compositions to be crystallized and does not refer to processes that occur during subsequent cooling of ingots. It may appear that a congruently solidifying composition of the solid solution demixes upon cooling. Precisely this takes place for, *e.g.*, lithium niobate in the $Li_2O-Nb_2O_5$ binary system. The congruently melting composition containing about 48 mol.% Li_2O, which corresponds to the melting-point maximum, demixes to eliminate $LiNb_3O_7$ below 910 °C (Svaasand's point).[53]

The solid solution in the CaF_2-BaF_2 system demixes in the same way, and thereby the composition of the minimum point is useless in the context of growing optical crystals.[69] For other $MF_2-M'F_2$ binary systems, the compositions of minima fall within the spinodal decomposition region, but the decomposition is very slow and does not preclude the practical use of the materials.

The materials corresponding to ternary saddle points are thermodynamically unstable under standard conditions, but no signs of decomposition have been noticed in them during a period of about a decade. In this respect, they resemble heterovalent solid solutions $M_{1-x}R_xF_{2+x}$.[63]

X. Constitutional undercooling stability of the liquid-solid interface in the vicinity of invariant points of ternary solid solutions

Given that certain conditions (Tiller's approximations [7, 82]) are fulfilled, in particular when the heat of crystallization is ignored, the constitutional undercooling stability of the liquid–solid interface in binary systems may be characterized by the simplest criterion,[7, 81] which is a generalization of Tiller's criterion:

$$\left(\frac{G}{R}\right) D \geqslant m\Delta x, \tag{10}$$

where G is the temperature gradient, R is the solidification rate, D is diffusivity, m is liquidus slope, and Δx is the concentration jump at the liquid–solid interface. This criterion is derived from the boundary condition on the crystal–melt interface and is applicable to unsteady-state

processes as well. When solidification is a quasi-equilibrium process, the right-hand side of inequality (10), which has the dimension of temperature and is referred to as stability function $F(x)$,[7] may be calculated from the phase diagram.[81] For constitutional undercooling to be suppressed, the ratio $(G/R)D$ should exceed some critical value; that is, it is necessary to reduce solidification rates and(or) increase temperature gradients, which is possible only to a certain limit.

If we assume that in the vicinity of a melting-point extreme for the solid solution at $x = x_0$ in a binary system liquidus and solidus curves can be fitted by parabolas $T_S = a(x - x_0)^2$ and $T_L = \alpha\, a(x - x_0)^2$, then it is easy to demonstrate[7] that the stability function is

$$F = 2\,a(\alpha - 1)(x - x_0)^2, \tag{11}$$

where a is constant and α is factor. Thus, the difficulties in growing a non-cellular crystal increase parabolically as the composition deviates from an invariant point.

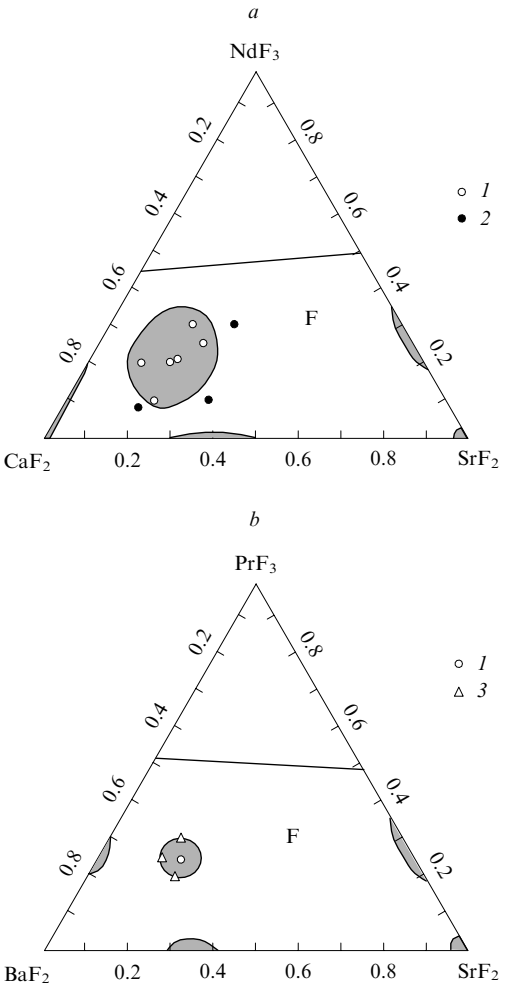


Figure 18. Fluorite solid solution (F) fields and stable Bridgman growth regions (shaded) in ternary systems: $CaF_2-SrF_2-NdF_3$ ($G = 30$ K cm^{-1}, $R = 5$ mm h^{-1})[86] (*a*); and $BaF_2-SrF_2-PrF_3$ ($G = 50$ K cm^{-1}, $R = 10$ mm h^{-1}) (*b*).
Experimental data: stable growth (*1*), cellular crystals (*2*) and nascent cells (*3*).

The general scheme of the appearance of constitutional undercooling in three-component solid solutions is the same as for two-component solid solutions (see Figs 3 *c*,*d*). The general stability criterion is written in the same way:

$$\left(\frac{G}{R}\right) \geqslant -\left(\frac{\Delta x_i}{D_i}\right)\left(\frac{\partial T^L}{\partial x_i}\right), \tag{12}$$

where D_i and Δx_i are, respectively, diffusion coefficient at point 1 and i-th component concentration jump at the liquid–solid interface; and $(\partial T^L/\partial x_i)$ is derivative along the diffusion path at the point corresponding to the melt composition.[83]

However, there is an obstacle to introducing the stability function for ternary systems: the diffusion trajectory that equalizes concentrations in the melt after they jump at the liquid–solid interface as a result of $k_i \neq 1$, does not coincide with the tie-line of postulated equilibrium at the crystal–melt interface (see Fig. 3 *e*).[84,85]

Although the strict introduction of the stability function, as it was done for binary systems, is impossible for ternary systems, it is yet evident that difficulties in growing high-quality crystals with deviation from the invariant point composition in a ternary system increase qualitatively in the same way as in a binary system. At the congruent melting point itself, $(\partial T^L/\partial x_i) = 0$ and $\Delta x_i = 0$.

Studies of the liquid–solid interface stability during growing fluorite solid solutions in the $CaF_2-SrF_2-NdF_3$,[86] $CaF_2-SrF_2-ErF_3$ and $BaF_2-SrF_2-PrF_3$ systems (Fig. 18) identified, for chosen G/R values, the concentration fields of planar growth in the vicinities of saddles points. Considerable sizes of these fields may serve to prove the advantages of saddle points; these advantages arise from the gentle-sloping liquidus and solidus surfaces, which change the sign of curvature in the vicinities of these points.

An appreciable shrinkage of the stability region of the liquid–solid interface in going from the $CaF_2-SrF_2-NdF_3$ system to the $BaF_2-SrF_2-PrF_3$ system may be interpreted as arising from the relatively small values of cation diffusivities in barium fluoride-based melts.[87]

XI. Instability of solidification at maximum and saddle points

When the constitutional undercooling instability of the liquid–solid interface is suppressed, cellular structures disappear, but striation appears in crystals. Photographs of a crystal grown at the boundary of the concentration region of the liquid–solid interface stability are found in Fig. 5 of the electronic appendix.

In the context of the constitutional undercooling stability of liquid–solid interface, maxima, minima, and saddles on the melting curves of binary solid solutions behave in the same manner. As regards concentration distribution along the crystal length, the situation is more complex. In what follows, we will understand the concentration stability of the growth process in mathematical terms as a characteristic of the behaviour of crystallization lines in a crystal–melt dynamic system. Mathematically, the only type of stable singular points is a stable node, *i.e.*, a minimum on melting curves (surfaces). Such a point has Lyapunov's asymptotic stability,[47,88] because there is a limiting point all trajectories tend to reach in its vicinity. In this case, the composition tends to restore the congruent one if occasionally deviating

from it during solidification. This behaviour looks like the existence in the system of a restoring force or a minimum of an energy function (an analogue of potential energy), which corresponds to a minimum point on melting surfaces. However, this is no more than analogy, for the reason that the initial sets of differential equations are not gradient ones and the relevant dynamic systems have not potentials.[89]

In cases of unstable nodes (maxima on melting surfaces), deviations will strengthen if the composition deviates from the congruent one during solidification. In cases of saddles, there is one selected line (separatrix) or (for higher-dimensional saddles) selected zero-thickness manifolds, on which the trajectories directed to the congruent composition lie. However, deviations from these manifolds direct the process trajectory bypass the congruent melting point in the concentration space. Thus, as well known, saddles are also unstable points.

The paradoxical conclusion that follows from the foregoing thermodynamic topological analysis consists in that, in the vast majority of cases, crystal growth is carried out from compositions that correspond to unstable points in the concentration space, namely, from unstable nodes (maxima on melting curves). This can be responsible for the systematical appearance in crystals of stria which correspond to concentration oscillations.[90, 91]

Thus, we should recognize why steady- or at least quasi-steady-state crystal growth arises from the unstable initial condition. This problem is opposite to the one to be usually solved in stability theory and catastrophe theory and in synergetics, namely, to recognize why and when a steady state or a steady-state process becomes unsteady [89] and can give rise to dissipative structures.[92]

Our suggestion consists in that striation in crystals is a consequence of oscillation processes, which are necessary for carrying out the steady-state growth of congruently melting crystals from the vicinity of an unstable point by directional solidification.[93] In other words, bifurcations of limit cycle generation in the concentration space should occur during crystal growth. For melting-point-curve maxima, the first such step is Andronov – Hopf bifurcation.[94, 95] For saddles, the situation is more complex. In this case, the simplest bifurcation is a separatrix-loop nonlocal bifurcation-1 commensurability (Fig. 19).[96, 97]

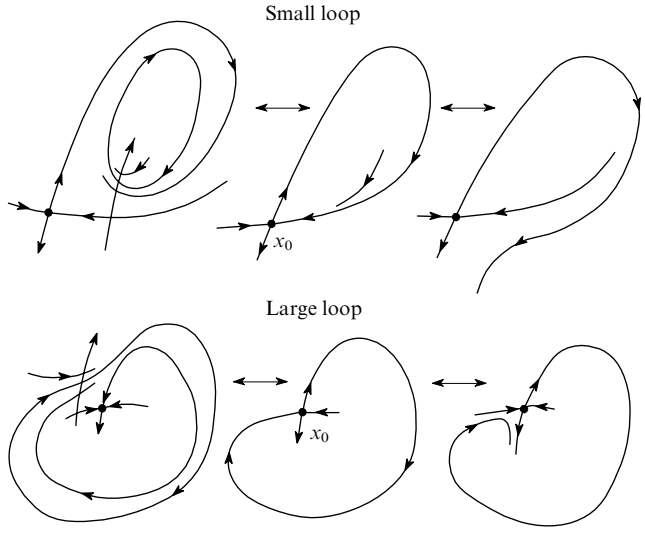


Figure 19. Bifurcation diagram and phase portraits for the separatrix loop bifurcation.

The key factors in bifurcation generation are apparently external impacts on the system, specifically, temperature jumps at the liquid – solid interface resulting from melt hydrodynamics (turbulent heat and mass transfer).

XII. Physical properties of crystals with compositions corresponding to saddle points

Tables 1 and 2 compile the compositions and some physical properties (unit cell parameters, melting points and thermal conductivities) for crystalline materials that correspond to saddle points in $SrF_2 - CaF_2 - RF_3$ and $SrF_2 - BaF_2 - RF_3$ ternary systems. Measurements were taken on single crystals that were melt-grown by vertical directional solidification under a fluorinating atmosphere. Thermal conductivities were measured by the absolute stationary longitudinal heat flux method in a temperature range of 50 – 300 K.[98]

Ion conductivity measurements in some compositions corresponding to the compositions of ternary saddle points in $SrF_2 - CaF_2 - RF_3$ systems [99, 100] showed insignificant deviations from the characteristics of heterovalent binary solid solutions. Refractive indices for materials can be derived from molecular or ionic refractions.

Comparative measurements showed the high efficiency of ytterbium active laser materials in the $CaF_2 - SrF_2 - YbF_3$ system [76] and the $BaF_2 - SrF_2 - YbF_3$ system.[101]

XIII. Prospects for multicomponent systems

The basic laws of solid solution crystallization remain the same as the chemical composition is becoming more complex. Addition of a fourth component to the composition corresponding to a ternary invariant point, in the general case, leads to incongruent melting. The increasing number

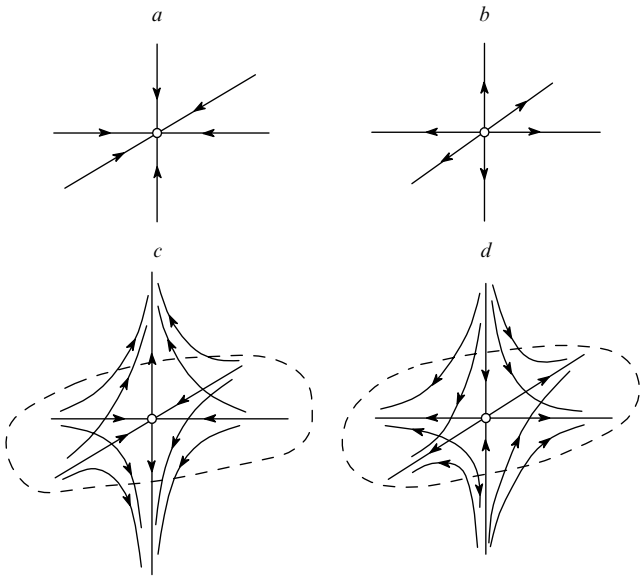


Figure 20. Suggested types of singular points corresponding to congruent melting of solid solutions in four-component systems: (*a*) melting-point minimum, (*b*) melting-point maximum and (*c*, *d*) saddles.

of components extends the range of possible invariant points due to the appearance of various types of multidimensional saddles. Figure 20 shows phase portraits in the vicinity of possible invariant points for four-component systems.

The thermodynamic theory of two-phase equilibria has been considered by Storonkin,[23] and thermodynamic topological analysis of invariant points in multicomponent systems has been reported [14, 16 102] for distillation phenomena and liquid–vapour equilibria. For quaternary systems, presentation is less clear, and for more complex systems it becomes unclear.

Attempts at finding a quaternary saddle in the $CaF_2-SrF_2-BaF_2-LaF_3$ system have not given an unambiguous answer. Figure 21 presents the development of

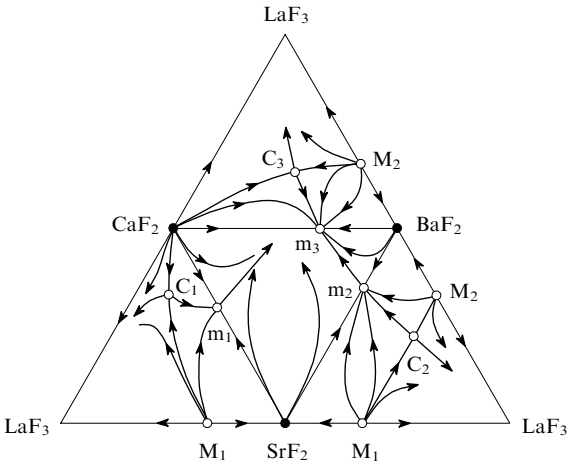


Figure 21. Development of phase portraits for the solidification of fluorite-type solid solutions in ternary subsystems of the $CaF_2-SrF_2-BaF_2-LaF_3$ four-component system constructed by the method proposed by Medvedev;[102] m_1, m_2 and m_3 are minima on the melting curves of binary solid solutions; M_1 and M_2 are maxima on the melting curves of binary solid solutions; C_1, C_2 and C_3 are saddles.

phase portraits of ternary subsystems of the aforementioned four-component system (*i.e.*, the development of the lateral surfaces of the tetrahedron on a plane). In the $CaF_2-SrF_2-LaF_3$ and $SrF_2-BaF_2-LaF_3$ systems, there are saddle points C_1 and C_2. In spite of the absence of a continuous solid solution between the components in the BaF_2-CaF_2 system, the saddle point C_3 does appear in the $CaF_2-BaF_2-LaF_3$ ternary system. The phase portrait of the $CaF_2-SrF_2-BaF_2$ system is outlined in accordance with our data.[103] This development may agree with various behaviours of crystallization lines inside the tetrahedron volume, specifically either with or without a four-component saddle (Fig. 22). Studies [103] do not allow us to clearly discriminate between the possible variants.

A congruent melting (stationary) point is likely to exist in the $CaO-Gd_2O_3-Ga_2O_3-ZrO_2$ four-component system within the primary separation field of the garnet phase.[104]

Multicomponent stationary points, as tangential and near-tangential phenomena, too, are becoming more and more rare and valuable as system's complexity increases. Let us assume that high-quality single crystals can be grown in the concentration vicinity ε of a stationary point. If so, it is natural to take that the measure of value of this point is

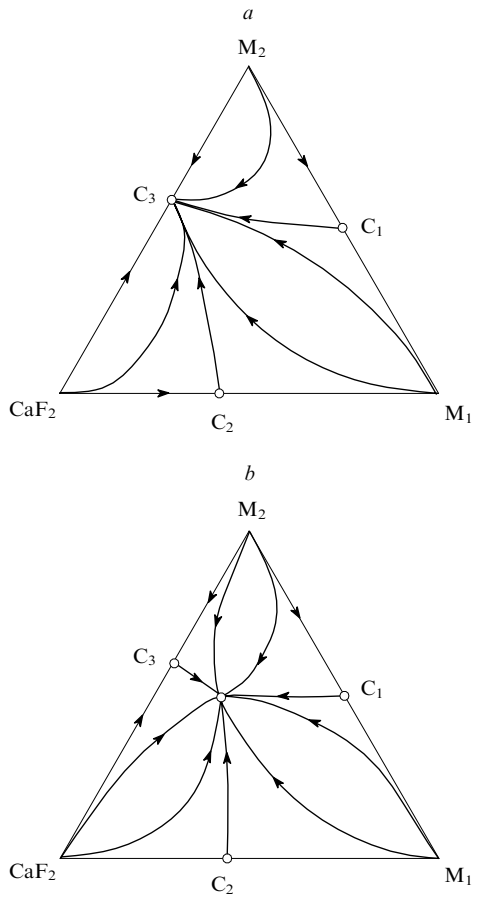


Figure 22. Two variants of a phase-portrait fragment for the solidification of fluorite solid solution in the $CaF_2-SrF_2-BaF_2-LaF_3$ four-component system on the separatrix surface that passes through CaF_2, C_1, M_1, C_2, M_2 and C_3 points: (*a*) without a quaternary point and (*b*) with a saddle quaternary point.

the ratio of the total volume of the concentration space to the volume of this vicinity. In a binary system, setting the entire concentration range equal to unity we obtain ε^{-1} to be the measure of the value of the stationary point. In a ternary system, this is a value reciprocal to the relative area of the vicinity ε . This value depends on the shape of the vicinity and amounts, for a unit side of the concentration triangle, for example, e^{-2} for a regular triangle with a side of ε and $\pi^{-1} \times 3^{0.5}\ \varepsilon^{-2}$ for a circle of diameter ε. Accordingly, for a four-component system the relative volume of the vicinity ε is ε^{-3} for a tetrahedral shape and $\pi^{-1} \times 2^{0.5}\ \varepsilon^{-3}$ for a sphere of diameter ε. Thus, we may conclude that the relative value of stationary points becomes greater as the number of components (n) increases as ε^{1-n}.

XIV. Conclusions

Our studies have demonstrated the potential of thermodynamic topological analysis for materials science purposes, namely, for design of new optical materials based on solid-solution compositions corresponding to saddle points on the liquidus surfaces of ternary systems. In $CaF_2-SrF_2-RF_3$, $SrF_2-BaF_2-RF_3$ and $PbF_2-CdF_2-RF_3$ systems, about 35 of such the points have been found; for 28, optical single crystals have been grown. The

$CaF_2-BaF_2-RF_3$ series remains to be studied, but we are sure that there are many saddle points in these systems, too.

Thermodynamic topological analysis allowed us to give a new look on the steadiness of solidification processes in the vicinity of congruent melting points and outline ways for controlling solidification processes. Of great interest is a comparative study of component distributions along the length in crystals grown from stable minimum points on the liquidus surface and from unstable points (maxima or saddles).

We are grateful to E V Zharikov, V I Kosyakov, L A Serafimov, P I Fedorov, V V Osiko and A A Chernov for fruitful discussions; V A Stasyuk, V A Konyushkin, S V Kuznetsov and A N Nakladov for growing crystals; P A Popov for measuring thermal conductivity; and V V Voronov for measuring unit cell parameters.

The review has been written with the financial support of the Russian Foundation for Basic Research (Project Nos 97-03-33306a, 04-03-32836 and 08-03-12080ofi) and the State Contract No. 02.740.11.0436 of September 30, 2009.

References

1. *Bulk Crystal Growth of Electronic, Optical and Optoelectronic Materials* (Ed. P Copper) (Chichester: Wiley, 2005)
2. *Springer Handbook of Crystal Growth* (Eds G Dhanaraj, K Byrappa, V Prasad, M Dudley) (Heidelberg, Dordrecht, London, New York: Springer, 2010)
3. S V Tsivinskii, A V Stepanov *Izv. Akad. Nauk SSSR, Ser. Neorg. Mater.* **2** 1177 (1966) [a]
4. L I Ivleva, N V Bogodaev, N M Polozkov, V V Osiko *Opt. Mater. (Amsterdam)* **4** 168 (1995)
5. RF P. 1800854 (1990)
6. I I Buchinskaya, P P Fedorov *Kristallografiya* **49** 333 (2004) [b]
7. P P Fedorov *Neorg. Mater.* **37** 95 (2001) [a]
8. Kh S Bagdasarov, in *Kristallokhimiya (Itogi Nauki i Tekhniki)* [Crystal Chemistry (Advances in Science and Engeneering Series)] (Moscow: Izd. VINITI, 1987) Vol. 21, p. 1
9. B P Sobolev, in *Rost Kristallov* (Growth of Crystals) (Moscow: Nauka, 1990) Vol. 18, p. 233
10. M Yu Sharonov, Z I Zhmurova, E A Krivandina, A A Bystrova, I I Buchinskaya, B P Sobolev *Opt. Commun.* **124** 558 (1996)
11. P P Fedorov, Doctoral Thesis in Chemical Sciences, Moscow Institute of Fine Chemical Technology, Moscow, 1991
12. F A H Schreinemakers *Z. Phys. Chem.* **36** 413 (1901)
13. Yu I Gurikov *Zh. Fiz. Khim.* **32** 1980 (1958) [c]
14. V T Zharov, L A Serafimov *Fiziko-khimicheskie Osnovy Distillyatsii i Rektifikatsii* (Physicochemical Foundations of Distillation and Rectification) (Leningrad: Khimiya, 1975)
15. L A Serafimov *Teoret. Osnovy Khim. Tekhnol.* **21** 74 (1987) [d]
16. L A Serafimov *Teoret. Osnovy Khim. Tekhnol.* **43** 274 (2009) [d]
17. L A Serafimov, A K Frolkova, T V Chelyuskina *Teoret. Osnovy Khim. Tekhnol.* **43** 648 (2009) [d]
18. F A H Schreinemakers *Z. Phys. Chem.* **52** 513 (1905)
19. P P Fedorov, in *Growth of Crystals* (Eds E I Givargizov, A M Melnicova) (New York, London: Consultants Bureau, 1996) Vol. 20, p. 103
20. L A Serafimov, V V Safonov *Zh. Neorg. Khim.* **45** 279 (2000) [e]
21. L A Serafimov, V V Safonov *Zh. Neorg. Khim.* **45** 682 (2000) [e]
22. L A Serafimov *Zh. Fiz. Khim.* **76** 1351 (2002) [c]
23. A V Storonkin *Termodinamika Geterogennykh Sistem* (Thermodynamics of Heterogeneous Systems) (Leningrad: Leningrad State University, 1967) Pts 1,2
24. L S Palatnik, A I Landau *Fazovye Ravnovesiya v Mnogokomponentnykh Sistemakh* (Phase Equilibria in Multicompanent Systems) (Khar'kov: Khar'kov University, 1961)
25. V P Zlomanov *R–T–x Diagrammy Dvukhkomponentnykh Sistem* (*R–T–x* Diagrams of Two-component Systems) (Moscow: Moscow State University, 1980)
26. P P Fedorov *Zh. Fiz. Khim.* **73** 1545 (1999) [c]
27. V Ya Anosov, S A Pogodin *Osnovnye Nachala Fiziko-khimicheskogo Analiza* (Basic Principles of Physicochemical Analysis) (Moscow, Leningrad: Academy of Sciences of the USSR, 1947)
28. A Andronov, L Pontryagin *Dokl. Akad. Nauk SSSR* **14** 247 (1937)
29. P P Fedorov *Zh. Neorg. Khim.* **49** 695 (2004) [a]
30. J Van-der-Waals, F Konstamm *Kurs Termostatiki* (Textbook of Thermodynamics) (Moscow: ONTI, 1936; translated from German) Pts 1, 2
31. J W Gibbs *Thermodynamics. Statistical Mechanics* (Moscow: Nauka, 1982; translated into Russian)
32. I N Bushmakin, I N Kim *Zh. Prikl. Khim.* **30** 200 (1957)
33. P P Fedorov, I I Buchinskaya, V A Stasyuk, O S Bondareva *Zh. Neorg. Khim.* **41** 464 (1996) [e]
34. I I Buchinskaya, Candidate Thesis in Chemical Sciences, Institute of Crystallography, Russian Academy of Sciences, Moscow, 1996
35. V A Stasyuk, I I Buchinskaya, N A Ust'yantseva, P P Fedorov *Zh. Neorg. Khim.* **43** 844 (1998) [e]
36. V A Stasyuk, I I Buchinskaya, P P Fedorov, V V Arbenina *Zh. Neorg. Khim.* **43** 1372 (1998) [e]
37. V A Stasyuk, Candidate Thesis in Chemical Sciences, Moscow Institute of Fine Chemical Technology, Moscow, 1998
38. P P Fedorov, N A Ivanovskaya, V A Stasyuk, I I Buchinskaya, B P Sobolev *Dokl. Akad. Nauk* **366** 500 (1999) [f]
39. P P Fedorov, I I Buchinskaya, V A Stasyuk, in *Fizika Kristallizatsii. K 100-letiyu Lemmleina* (The Physics of Crystallisation. To Lemmlein Centenary) (Moscow: Fizmatlit, 2002) p. 220
40. R Vögel *Die Heterogenen Gleichgewichte* (Leipzig: Akademische Verlagsgesellschaft, 1959)
41. V G Kuznetsov, K K Palkina *Zh. Neorg. Khim.* **8** 1204 (1963) [e]
42. P P Fedorov *Zh. Neorg. Khim.* **52** 122 (2007) [e]
43. W G Pfann *Zone Melting* (New York, London, Sydney: Wiley, 1966)
44. V I Kosyakov *Geol. Geofiz.* **39** 1242 (1998) [g]
45. N N Bautin, E A Leontovich *Metody i Priemy Kachestvennogo Issledovaniya Dinamicheskikh Sistem na Ploskosti* (Methods and Techniques of the Qualitative Study of Dynamical Systems on the Plane) (Moscow: Nauka, 1976)
46. D K Arrowsmith, C M Place *Ordinary Differential Equations. A Qualitative Approach with Applications* (London, New York: Chapman and Hall, 1982)
47. V I Arnold *Ordinary Differential Equations* (Berlin: Springer, 1992; translated from Russian)
48. H S Yoder, C T Tilley *Origin of Basalt Magmas* [*J. Petrology* **3** (Part J) 342 (1962)]
49. *Diagrammy Plavkosti Solevykh Sistem. Spravochnik* (Fusion Diagrams of Salt Systems. Handbook) (Eds V I Posypaiko, E A Alekseeva) (Moscow: Metallurgiya, 1977) Pt. 3
50. A A Volykhov, L V Yashina, V I Shtanov *Neorg. Mater.* **46** 532 (2010) [a]
51. A T Grigor'ev, L A Panteleimonov, E M Sokolovskaya *Izv. Sektora Fiz.-khim. Analiza* **27** 185 (1956)
52. A Dakki, M Ferriol, M-T Cohen-Adad *Eur. J. Solid State Inorg. Chem.* **33** 19 (1996)
53. L O Svaasand, M Eriksrud, G Nakken, A P Grande *J. Cryst. Growth* **22** 230 (1974)
54. N P Got'ko, V V Kirilenko, V F Churbakov, R N Shchelokov *Izv. Akad. Nauk SSSR, Ser. Neorg. Mater.* **22** 1438 (1986) [a]
55. L A Ol'khovaya, G A Karpenko, D D Ikrami, P P Fedorov *Zh. Neorg. Khim.* **36** 2919 (1991) [e]
56. P P Fedorov, A V Rappo *Zh. Neorg. Khim.* **53** 1210 (2008) [e]

57. P P Fedorov, I I Buchinskaya, L A Serafimov *Zh. Neorg. Khim.* **47** 1371 (2002) [e]
58. B P Sobolev, P P Fedorov, N L Tkachenko, K B Seiranyan, A M Kevorkov, Kh S Bagdasarov, V S Sidorov, D D Ikrami, in *Issledovanie Materialov dlya Opticheskikh Pokrytii. Trudy VNII Lyuminoforov* (Investigation of Materials for Optical Coatings. Proceedings of All-Union Research Institute of Luminophors, Stavropol', 1977) No. 15, p. 73
59. E V Zharikov, A I Zagumennyi, S N Kozlikin, S V Lavrishchev, G B Lutts *Dokl. Akad. Nauk SSSR* **308** 1166 (1989) [f]
60. A L Denisov, E V Zharikov, A I Zagumennyi, S N Kozlikin, S V Lavrishchev, G B Lutts, S A Samoilova *Osobennosti Izomorfnogo Zameshcheniya v Ittrii – Sskandii – Alyuminievom Granate* (Isomorphous Substitutions in Yttrium – Scandium – Aluminium Garnet) Preprint of Institute of General Physics, Russian Academy of Sciences, 1989, No. 58
61. A L Denisov, E V Zharikov, A I Zagumennyi, S N Kozlikin, S V Lavrishchev, G B Lutts, S A Samoilova *Trudy IOFAN (Proceedings of the A M Prokhorov General Physics Institute)* **26** 98 (1990)
62. B P Sobolev *The Rare Earth Trifluorides. The High-temperature Chemistry of the Rare Earth Trifluorides* Pt. 1 (Barcelona: Institut d'Estudis Catalans, 2000)
63. P P Fedorov *Russ. J. Inorg. Chem.* **45** S268 (2000)
64. J T Mouchovski, K A Temelkov, N K Vuchkov *Prog. Cryst. Growth Characteriz. Mater.* **57** 1 (2011)
65. D Klimm, M Rabe, R Bertram, R Uecker, L Parthier *J. Cryst. Growth* **310** 152 (2008)
66. H R Nafziger *J. Am. Ceram. Soc.* **54** 467 (1971)
67. A de Kozak, M Samouel, A Chretien *Rev. Chim. Miner.* **8** 805 (1971)
68. I I Buchinskaya, P P Fedorov *Europhys. Lett.* **83** 16001 (2008)
69. P P Fedorov, I I Buchinskaya, N A Ivanovskaya, V V Konovalova, S V Lavrishchev, B P Sobolev *Dokl. Akad. Nauk* **401** 652 (2005) [f]
70. P P Fedorov, L V Medvedeva *Zh. Neorg. Khim.* **34** 2674 (1989) [e]
71. V J Fratello, C D Brandle, A J Valentino *J. Cryst. Growth* **80** 26 (1987)
72. T Tanaka, S Otani, Y Ishizawa *J. Cryst. Growth* **99** 994 (1990)
73. S-Q Wang, J Harada, S Uda *J. Cryst. Growth* **219** 263 (2000)
74. H Takeda, K Shimamura, V I Chani, T Fukuda *J. Cryst. Growth* **197** 204 (1999)
75. N I Sorokin, I I Buchinskaya, B P Sobolev *Zh. Neorg. Khim.* **37** 2653 (1992) [e]
76. Yu P Grigorash, Candidate Thesis in Chemical Sciences, Moscow, Moscow State University, 1981
77. T T Basiev, S V Vasil'ev, M E Doroshenko, V A Konyushkin, S V Kuznetsov, V V Osiko, P P Fedorov *Kvant. Elektron.* **37** 934 (2007) [h]
78. P P Fedorov, V V Osiko, in *Bulk Crystal Growth of Electronic, Optical and Optoelectronic Materials* (*Wiley Series in Materials for Electronic and Optoelectronic Applications*) (Ed. P Capper) (Chichester: Wiley: 2005) p. 339
79. I I Buchinskaya, P P Fedorov, V A Konushkin, S V Kuznetsov, in *International Conference 'Crystal Materials 2005' (ICCM|2005) (Abstracts), Kharkov, Ukraine, 2005* p. 24
80. T T Basiev, I I Buchinskaya, S V Vasil'ev, S V Kuznetsov, V A Konyushkin, A N Nakladov, V V Osiko, P P Fedorov, in *XII Natsional'naya Konferentsiya po Rostu Kristallov (Tezisy Dokladov)* [The XIIth National Conference on Crystal Growth (Abstracts of Reports), Moscow, 2006] p. 237
81. S V Kuznetsov, Candidate Thesis in Chemical Sciences, Moscow Institute of Fine Chemical Technology, Moscow, 2007
82. P P Fedorov, T M Turkina, V A Meleshina, B P Sobolev, in *Rost Kristallov* (Crystal Growth) (Moscow: Nauka, 1988) Vol. 17, p. 198
83. P P Fedorov, in *X Natsional'naya Konferentsiya po Rostu Kristallov (Tezisy Dokladov)* [The Xth National Conference on Crystal Growth (Abstracts of Reports), Moscow, 2002] p. 38
84. J S Kirkaldy, D J Young *Diffusion in the Condensed State* (London: Institute of Metals, 1987)
85. W D Hoppe, J E Morral *Acta Metall. Mater.* **42** 3887 (1994)
86. P P Fedorov, V A Stasyuk, N A Ivanovskaya, I I Buchinskaya, S V Isaev, A G Papashvili *Dokl. Akad. Nauk* **369** 217 (1999) [f]
87. S V Kuznetsov, P P Fedorov *Inorg. Mater.* **44** 1434 (2008)
88. A A Andronov, E A Leontovich, I I Gordon, A G Maier *Kachestvennaya Teoriya Dinamicheskikh Sistem Vtorogo Poryadka* (Qualitative Theory of Second-order Dynamic Systems) (Moscow: Nauka, 1966)
89. R Gilmore *Catastrophe Theory for Scientists and Engineers* (New York: Wiley, 1981)
90. V A Meleshina, P P Fedorov *Dokl. Akad. Nauk* **364** 498 (1999) [f]
91. P P Fedorov, A A Bystrova, V A Meleshina, E V Zharikov, in *Atlas Vremennykh Variatsii Prirodnykh, Antropogennykh i Sotsial'nykh Protsessov* (Atlas of Temporal Variations of Natural, Anthropogenic and Social Processes) (Moscow: Nauchnyi Mir, 2002) Vol. 3, p. 612
92. G Nikolis, I Prigogine *Self-Organization in Nonequilibrium Systems* (New York:Wiley, 1977)
93. P P Fedorov *Zh. Neorg. Khim.* **50** 2059 (2005) [e]
94. A A Andronov, E A Leontovich, I I Gordon, A G Maier *Theory of Bifurcations of Dynamic Systems on a Plane* (New York: Wiley, 1973)
95. J Marsden, M McCracken *The Hopf Bifurcation and Its Applications* (Heidelberg: Springer, 1976)
96. V I Arnol'd, V S Afraimovich, Yu S Il'yashenko, L P Shil'nikov, in *Sovremennye Problemy Matematiki. Fundamental'nye Napravleniya (Itogi Nauki i Tekhniki)* [Modern Problems of Mathematics. Basic Research (Advances in Science and Engeneering Series)] (Moscow: Izd. VINITI, 1986) Vol. 5
97. E Leontovich *Dokl. Akad. Nauk SSSR* **78** 641 (1951)
98. N N Sirota, P A Popov, I A Ivanov *Cryst. Res. Technol.* **27** 535 (1992)
99. I I Buchinskaya, V Trnovtsova, V A Stasyuk, P P Fedorov, in *X Simpozium po Khimii Neorganicheskikh Ftoridov. Ftoridnye Materialy (Tezisy Dokladov)* [The Xth Symposium on Chemistry of Inorganic Fluorides (Abstracts of Reports), Moscow, 1998] p. 27
100. N I Sorokin, D N Karimov, E A Krivandina, Z I Zhmurova, O N Komar'kova *Kristallografiya* **53** 297 (2008) [b]
101. O K Alimov, T T Basiev, M E Doroshenko, P P Fedorov, V A Konyushkin, S V Kouznetsov, A N Nakladov, V V Osiko, O V Shlyakhova, in *Advanced Solid State Photonics (ASSP-2008) (Conference Program and Technical Digest), Nara, Japan, 2008* MC13
102. D V Medvedev, Candidate Thesis in Technical Sciences, Moscow M V Lomonosov State University of Fine Chemical Technology, Moscow, 2011
103. P P Fedorov, I I Buchinskaya, V V Konovalova, R M Zakalyukin, in *Trudy Vtorogo Mezhdunarodnogo Sibirskogo Seminara 'Sovremennye Neorganicheskie Ftoridy' (INTERSIBFLUORINE -2006)* [Proceedings of Second International Siberian Seminar 'Modern Inorganic Fluorides', Tomsk, 2006] p. 315
104. D Mateika, J Herrnring, R Rath, C Rusche *J. Cryst. Growth* **30** 311 (1975)

[a] — *Inorg. Mater. (Engl. Transl.)*
[b] — *Crystallogr. Rep. (Engl. Transl.)*
[c] — *Russ. J. Phys. Chem., Ser. A (Engl. Transl.)*
[d] — *Theor. Found. Chem. Eng. (Engl. Transl.)*
[e] — *Russ. J. Inorg. Chem. (Engl. Transl.)*
[f] — *Dokl. Phys. Chem. (Engl. Transl.)*
[g] — *Russ. Geol. Geophys. (Engl. Transl.)*
[h] — *Quant. Electron. (Engl. Transl.)*